
Active Slices for Sliced Stein Discrepancy

Wenbo Gong¹ Kaibo Zhang¹ Yingzhen Li² José Miguel Hernández-Lobato¹

Abstract

Sliced Stein discrepancy (SSD) and its kernelized variants have demonstrated promising successes in goodness-of-fit tests and model learning in high dimensions. Despite their theoretical elegance, their empirical performance depends crucially on the search of optimal slicing directions to discriminate between two distributions. Unfortunately, previous gradient-based optimisation approaches for this task return sub-optimal results: they are computationally expensive, sensitive to initialization, and they lack theoretical guarantees for convergence. We address these issues in two steps. First, we provide theoretical results stating that the requirement of using optimal slicing directions in the kernelized version of SSD can be relaxed, validating the resulting discrepancy with *finite* random slicing directions. Second, given that good slicing directions are crucial for practical performance, we propose a fast algorithm for finding such slicing directions based on ideas of active sub-space construction and spectral decomposition. Experiments on goodness-of-fit tests and model learning show that our approach achieves both improved performance and faster convergence. Especially, we demonstrate a 14-80x speed-up in goodness-of-fit tests when comparing with gradient-based alternatives.

1. Introduction

Discrepancy measures between two distributions are critical tools in modern statistical machine learning. Among them, *Stein discrepancy* (SD) and its kernelized version, kernelized Stein discrepancy (KSD), have been extensively used for *goodness-of-fit* (GOF) testing (Liu et al., 2016; Chwialkowski et al., 2016; Huggins & Mackey, 2018; Jitkrit-

tum et al., 2017; Gorham & Mackey, 2017) and model learning (Liu & Wang, 2016; Pu et al., 2017; Hu et al., 2018; Grathwohl et al., 2020). Despite their recent success, applications of Stein discrepancies to high-dimensional distribution testing and learning remains an unsolved challenge.

These “curse of dimensionality” issues have been recently addressed by the newly proposed Sliced Stein discrepancy (SSD) and its kernelized variants SKSD (Gong et al., 2021), which have demonstrated promising results in both high dimensional GOF tests and model learning. They work by first projecting the score function and the test inputs across two slice directions r and g_r , and then comparing the two distributions using the resulting one dimensional slices. The performance of SSD and SKSD crucially depends on choosing slicing directions that are highly discriminative. Indeed, Gong et al. (2021) showed that such discrepancy can still be valid despite the information loss caused by the projections, if *optimal slices* – directions along which the two distributions differ the most – are used. Unfortunately, gradient-based optimization for searching such optimal slices often suffers from slow convergence and sub-optimal solutions. In practice, many gradient updates may be required to obtain a reasonable set of slice directions (Gong et al., 2021).

We aim to tackle the above practical challenges by proposing an efficient algorithm to find *good* slice directions with statistical guarantees. Our contributions are as follows:

- We propose a computationally efficient variant of SKSD using a *finite number of random slices*. This relaxes the restrictive constraint of having to use *optimal* slices, with the consequence that convergence during optimisation to a global optimum is no longer required.
- Given that *good* slices are still preferred in practice, we propose surrogate optimization tasks to find such directions. These are called *active slices* and have analytic solutions that can be computed very efficiently.
- Experiments on GOF test benchmarks (including testing on restricted Boltzmann machines) show that our algorithm outperforms alternative gradient-based approaches while achieving at least a 14x speed-up.
- In the task of learning high dimensional *independent component analysis* (ICA) models (Comon, 1994), our algorithm converges much faster and to significantly better solutions than other baselines.

¹Department of Engineering, University of Cambridge, Cambridge, United Kingdom ²Department of Computing, Imperial College London, London, United Kingdom. Correspondence to: Wenbo Gong <wg242@cam.ac.uk>, José Miguel Hernández-Lobato <jmh233@cam.ac.uk>.

Road map: First, we give a brief background for SD , $SKSD$ and its relevant variants (Section 2). Next, we show that the optimality of slices are not necessary. Instead, finite random slices are enough to ensure the validity of $SKSD$ (3.1). Despite that relaxing the optimality constraint gives us huge freedom to select slice directions, choosing an appropriate objective for finding slices is still crucial. Unfortunately, analysing $SKSD$ in RKHS is challenging. We thus propose to analyse SSD as a surrogate objective by showing $SKSD$ can be well approximated by SSD (Section 3.2). Lastly, by analyzing SSD , we propose algorithms to find active slices for $SKSD$ (Sections 4, 5, 6), and demonstrate the efficacy of our proposal in the experiments (Section 7). Assumptions and proofs of theoretical results as well as the experimental settings can be found in the appendix.

2. Background

For a distributions p on $\mathcal{X} \subset \mathbb{R}^D$ with differentiable density, we define its score function as $\mathbf{s}_p(\mathbf{x}) = \nabla_{\mathbf{x}} \log p(\mathbf{x})$. We also define the Stein operator \mathcal{A}_p for distribution p as

$$\mathcal{A}_p \mathbf{f}(\mathbf{x}) = \mathbf{s}_p(\mathbf{x})^T \mathbf{f}(\mathbf{x}) + \nabla_{\mathbf{x}}^T \mathbf{f}(\mathbf{x}), \quad (1)$$

where $\mathbf{f} : \mathcal{X} \rightarrow \mathbb{R}^D$ is a test function. Then the *Stein discrepancy* (SD) (Gorham & Mackey, 2015) between two distributions p, q with differentiable densities on \mathcal{X} is

$$D_{SD}(q, p) = \sup_{\mathbf{f} \in \mathcal{F}_q} \mathbb{E}_q[\mathcal{A}_p \mathbf{f}(\mathbf{x})], \quad (2)$$

where \mathcal{F}_q is the Stein’s class of q that contains test functions satisfying $\mathbb{E}_q[\mathcal{A}_q \mathbf{f}(\mathbf{x})] = 0$ (also see Definition B.2 in appendix B). The supremum can be obtained by choosing $\mathbf{f}^* \propto \mathbf{s}_p(\mathbf{x}) - \mathbf{s}_q(\mathbf{x})$ if \mathcal{F}_q is rich (Hu et al., 2018).

Chwialkowski et al. (2016); Liu et al. (2016) further restricts the test function space \mathcal{F}_q to be a unit ball in an RKHS induced by a c_0 -universal kernel $k : \mathcal{X} \times \mathcal{X} \rightarrow \mathbb{R}$. This results in the *kernelized Stein discrepancy* (KSD), which can be computed analytically:

$$D^2(q, p) = \left(\sup_{\mathbf{f} \in \mathcal{H}_k, \|\mathbf{f}\|_{\mathcal{H}_k} \leq 1} \mathbb{E}_q[\mathcal{A}_p \mathbf{f}(\mathbf{x})] \right)^2 \quad (3)$$

$$= \|\mathbb{E}_q[\mathbf{s}_p(\mathbf{x})k(\mathbf{x}, \cdot) + \nabla_{\mathbf{x}} k(\mathbf{x}, \cdot)]\|_{\mathcal{H}_k}^2,$$

where \mathcal{H}_k is the k induced RKHS with norm $\|\cdot\|_{\mathcal{H}_k}$.

2.1. Sliced kernelized Stein discrepancy

Despite the theoretical elegance of KSD , it often suffers from the curse-of-dimensionality in practice. To address this issue, Gong et al. (2021) proposed a divergence family called *sliced Stein discrepancy* (SSD) and its kernelized variants, under mild assumptions on the regularity of probability densities (Assumptions 1-4 in appendix B) and the

richness of the kernel (Assumption 5 in appendix B). The key idea is to compare the distributions on their one dimensional slices by projecting the score \mathbf{s}_p and test input \mathbf{x} with two directions \mathbf{r} and its corresponding \mathbf{g}_r , respectively. Readers are referred to appendix C for details. Despite that one cannot access all the information possessed by \mathbf{s}_p and \mathbf{x} due to the projections, the validity of the discrepancy can be ensured by using an orthogonal basis for \mathbf{r} along with the corresponding most discriminative \mathbf{g}_r directions. The resulting valid discrepancy is called *maxSSD-g*, which uses a set of orthogonal basis $\mathbf{r} \in O_r$ and their corresponding optimal \mathbf{g}_r directions:

$$S_{\max_{g_r}}(q, p) = \sum_{\mathbf{r} \in O_r} \sup_{\substack{h_{r g_r} \in \mathcal{F}_q \\ \mathbf{g}_r \in \mathbb{S}^{D-1}}} \mathbb{E}_q[s_p^T(\mathbf{x})h_{r g_r}(\mathbf{x}^T \mathbf{g}_r) + \mathbf{r}^T \mathbf{g}_r \nabla_{\mathbf{x}^T \mathbf{g}_r} h_{r g_r}(\mathbf{x}^T \mathbf{g}_r)], \quad (4)$$

where $h_{r g_r} : \mathcal{K} \subseteq \mathbb{R} \rightarrow \mathbb{R}$ is the test function, \mathbb{S}^{D-1} is the D -dimensional unit sphere and $s_p^r(\mathbf{x}) = \mathbf{s}_p(\mathbf{x})^T \mathbf{r}$ is the projected score function. Under certain scenarios (Gong et al., 2021), i.e. GOF test, one can further improve the performance of *maxSSD-g* by replacing $\sum_{\mathbf{r} \in O_r}$ with the optimal $\sup_{\mathbf{r} \in \mathbb{S}^{D-1}}$ in Eq.4, resulting in another variant called *maxSSD-rg* ($S_{\max_{r g_r}}$). This increment in performance is due to the higher discriminative power provided by the optimal \mathbf{r} .

However, the optimal test functions $h_{r g_r}^*$ in *maxSSD-g* (or *-rg*) are intractable in practice. Gong et al. (2021) further proposed kernelized variants to address this issue by letting \mathcal{F}_q to be in a unit ball of an RKHS induced by a c_0 -universal kernel $k_{r g_r}$. With

$$\xi_{p, r, g_r}(\mathbf{x}, \cdot) = s_p^T(\mathbf{x})k_{r g_r}(\mathbf{x}^T \mathbf{g}_r, \cdot) + \mathbf{r}^T \mathbf{g}_r \nabla_{\mathbf{x}^T \mathbf{g}_r} k_{r g_r}(\mathbf{x}^T \mathbf{g}_r, \cdot), \quad (5)$$

the *maxSKSD-g* (the kernelized version of *maxSSD-g*) is

$$SK_{\max_{g_r}}(q, p) = \sum_{\mathbf{r} \in O_r} \sup_{\mathbf{g}_r \in \mathbb{S}^{D-1}} \|\mathbb{E}_q[\xi_{p, r, g_r}(\mathbf{x})]\|_{\mathcal{H}_{r g_r}}^2, \quad (6)$$

where $\mathcal{H}_{r g_r}$ is the RKHS induced by $k_{r g_r}$ with the associated norm $\|\cdot\|_{\mathcal{H}_{r g_r}}$. Similarly, a kernelized version of *maxSSD-rg*, denoted by *maxSKSD-rg* ($SK_{\max_{r g_r}}$), is obtained by replacing $\sum_{\mathbf{r} \in O_r}$ with $\sup_{\mathbf{r} \in \mathbb{S}^{D-1}}$ in Eq.6.

Despite that *maxSKSD-g* (or *-rg*) addresses the tractability of test functions, the practical challenge of computing them is the computation of the optimal slice directions \mathbf{r} and \mathbf{g}_r . Gradient-based optimization (Gong et al., 2021) for such computation suffers from slow convergence; even worse, it is sensitive to initialization and returns sub-optimal solutions only. In such case, it is unclear whether the resulting discrepancy is still valid, making the correctness of GOF test unverified. Therefore, the first important question to

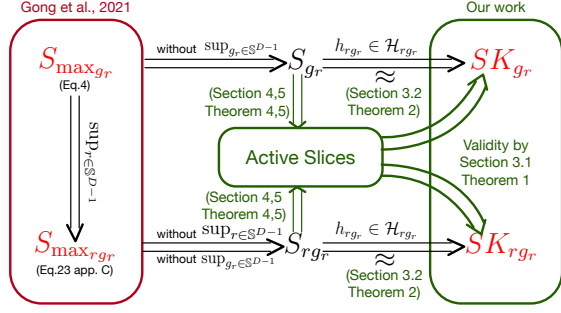


Figure 1. The relationship between different SSD discrepancies, where green texts indicate our contributions, red symbols indicate valid discrepancies and $\mathcal{H}_{r g_r}$ is the RKHS induced by kernel $k_{r g_r}$. The leftmost part are the discrepancies proposed by Gong et al. (2021), whereas the rightmost part + central “Active Slices” are our contributions. The arrows \Rightarrow indicate the connections between Gong et al. (2021) and our work.

ask is: are the optimality of slices a necessary condition for the validity of $maxSKSD-g$ (or $-rg$)? Remarkably, we show that the answer is **No** with mild assumptions on the kernel (**Assumption 5-6** in appendix B).

As the sliced Stein discrepancy defined previously involves a sup operator, making them difficult to analyze, we need to define notations for their “sub-optimal” versions. For example, $maxSSD-g$ (Eq.4) involves a sup operator over slices g_r . We thus define $SSD-g$ (S_{g_r}) as Eq.4 with a given g_r instead of the sup:

$$S_{g_r} = \sum_{r \in O_r} \sup_{h_{r g_r} \in \mathcal{F}_q} \mathbb{E}_q [s_p^r(\mathbf{x}) h_{r g_r}(\mathbf{x}^T \mathbf{g}_r) + \mathbf{r}^T \mathbf{g}_r \nabla_{\mathbf{x}^T \mathbf{g}_r} h_{r g_r}(\mathbf{x}^T \mathbf{g}_r)] \quad (7)$$

Following similar logic, we define the “sub-optimal” version for each of the discrepancy mentioned in this section as table 1 and appendix A.

3. Relaxing constraints for the SKSD family

3.1. Is optimality necessary for validity?

As mentioned before, the discrepancy validity of max SKSD requires the optimality of slice directions, which restricts its application in practice. In the following, we show that these restrictions can be much relaxed with mild assumptions on the kernel. All proofs can be found in Appendix E.

The key idea is to use kernels such that the corresponding term $SK_{r g_r}$ is *real analytic* w.r.t. both \mathbf{r} and \mathbf{g}_r , which is detailed by **Assumption 6** (Appendix B). A nice property of any real analytic function is that, unless it is a constant function, otherwise the set of its roots has zero Lebesgue measure. This means the possible valid slices are almost

everywhere in \mathbb{R}^D , giving us huge freedom to choose slices without worrying about violating validity.

Theorem 1 (Conditions for valid slices). *Assuming assumptions 1-4 (density regularity), 5 (richness of kernel) and 6 (real analytic kernel) in Appendix B, let $g_r \sim \eta_g$ for each $r \sim \eta_r$, where η_g, η_r are distributions on \mathbb{R}^D with a density, then $SK_{r g_r}(q, p) = 0$ iff. $p = q$ almost surely.*

The above theorem tells us that a *finite* number of *random* slices is enough to make $SK_{r g_r}$ valid without the need of using optimal slices (c.f. $SK_{\max_{r g_r}}$). In practice, we often consider $\mathbf{r}, \mathbf{g}_r \in \mathbb{S}^{D-1}$ instead of \mathbb{R}^D . Fortunately, one can easily transform arbitrary slices to \mathbb{S}^{D-1} without violating the validity. For any \mathbf{r}, \mathbf{g}_r , we (i) add Gaussian noises to them, and (2) re-normalize the noisy \mathbf{r}, \mathbf{g}_r to unit vectors. We refer to corollary 6.1 in appendix E.1 for details.

3.2. Relationship between SSD and SKSD

Theorem 1 allows us to use random slices. However, it is still beneficial to find good ones in practice. Unfortunately, $SK_{r g_r}$ is not a suitable objective for finding good slice directions. This is because, unlike the test function in a general function space ($h_{r g_r} \in \mathcal{F}_q$), the optimal kernel test function ($\mathbb{E}_q[\xi_{p, r, g_r}(\mathbf{x}, \cdot)]$) can not be easily analyzed for finding good slices due to its restriction in RKHS.

Instead, we propose to use S_g (or $S_{r g_r}$) as the optimization objective. To justify $S_{r g_r}$ as a good replacement for SK_{g_r} , we show that $SK_{r g_r}$ approximates $S_{r g_r}$ arbitrarily well if the corresponding RKHS of the chosen kernel is dense in continuous function space. Similar results for $SK_g \approx S_g$ can be derived accordingly as the only difference between S_{g_r} and $S_{r g_r}$ is the summation over orthogonal basis O_r . However, $S_{r g_r}$ still involves a sup operator over test functions $h_{r g_r}$, which hinders further analysis. To deal with this, we give an important proposition that are needed in almost every theoretical claims we made. This proposition characterises the optimal test functions for $S_{r g_r}$ (or S_{g_r}).

Proposition 1 (Optimal test function given \mathbf{r}, \mathbf{g}_r). *Assume assumptions 1-4 (density regularity) and given directions \mathbf{r}, \mathbf{g}_r . Assume an arbitrary orthogonal matrix $\mathbf{G}_r = [\mathbf{a}_1, \dots, \mathbf{a}_D]^T$ where $\mathbf{a}_i \in \mathbb{S}^{D \times 1}$ and $\mathbf{a}_d = \mathbf{g}_r$. Denote $\mathbf{x} \sim q$ and $\mathbf{y} = \mathbf{G}_r \mathbf{x}$ which is also a random variable with the induced distribution q_{G_r} . Then, the optimal test function for $S_{r g_r}$ is*

$$h_{r g_r}^*(\mathbf{x}^T \mathbf{g}_r) \propto \mathbb{E}_{q_{G_r}(\mathbf{y}_{-d} | y_d)} [(s_p^r(\mathbf{G}_r^{-1} \mathbf{y}) - s_q^r(\mathbf{G}_r^{-1} \mathbf{y}))] \quad (8)$$

where $y_d = \mathbf{x}^T \mathbf{g}_r$ and \mathbf{y}_{-d} contains other \mathbf{y} elements.

Intuitively, assume \mathbf{G}_r is a rotation matrix. Then $h_{r g_r}^*$ is the conditional expected score difference between two rotated p and q . This form is very similar to the optimal test function for SD, which is just the score difference between the origi-

Table 1. Notations for “sub-optimal” versions of SSD & SKSD.

Optimal form	$\max_{\mathbf{g}_r} \text{SSD-g} (S_{\max_{\mathbf{g}_r}})$	$\max_{\mathbf{r}, \mathbf{g}_r} \text{SSD-rg} (S_{\max_{\mathbf{r}, \mathbf{g}_r}})$	$\max_{\mathbf{g}_r} \text{SKSD-g} (SK_{\max_{\mathbf{g}_r}})$	$\max_{\mathbf{r}, \mathbf{g}_r} \text{SKSD-rg} (SK_{\max_{\mathbf{r}, \mathbf{g}_r}})$
Modifications	Change $\sup_{\mathbf{g}_r}$ to given \mathbf{g}_r in Eq.4	Change $\sup_{\mathbf{r}, \mathbf{g}_r}$ to given \mathbf{r}, \mathbf{g}_r in Eq.37 (App. C)	Same as $\max_{\mathbf{g}_r} \text{SSD-g}$ in Eq.6	Same as $\max_{\mathbf{r}, \mathbf{g}_r} \text{SSD-rg}$ in Eq.41 (App. C)
“sub-optimum”	$\text{SSD-g} (S_{\mathbf{g}_r})$	$\text{SSD-rg} (S_{\mathbf{r}, \mathbf{g}_r})$	$\text{SKSD-g} (SK_{\mathbf{g}_r})$	$\text{SKSD-rg} (SK_{\mathbf{r}, \mathbf{g}_r})$

nal p, q . Knowing the optimal form of h_{r, \mathbf{g}_r}^* , we can show SK_{r, \mathbf{g}_r} can be well approximated by S_{r, \mathbf{g}_r} .

Theorem 2 ($SK_{r, \mathbf{g}_r} \approx S_{r, \mathbf{g}_r}$). *Assume assumptions 1-4 (density regularity) and 5 (richness of kernel). Given \mathbf{r} and $\mathbf{g}_r, \forall \epsilon > 0$ there exists a constant C such that*

$$0 \leq S_{r, \mathbf{g}_r} - SK_{r, \mathbf{g}_r} < C\epsilon.$$

As S_{r, \mathbf{g}_r} approximates SK_{r, \mathbf{g}_r} arbitrary well, the hope is that good slices for S_{r, \mathbf{g}_r} also correspond to good slices for SK_{r, \mathbf{g}_r} in practice. Therefore in the next section we focus on analyzing S_{r, \mathbf{g}_r} instead to propose an efficient algorithm for finding good slices.

4. Active slice direction \mathbf{g}_r

Finding good slices involves alternating maximization of \mathbf{r} and \mathbf{g}_r . To simplify the analysis, we focus on good directions \mathbf{g}_r given fixed \mathbf{r} , e.g. the orthogonal basis $\mathbf{r} \in O_r$ for now. Finding good \mathbf{g}_r is achieved in two steps: (i) Rewriting the problem of the maximizing $S_{\mathbf{g}_r}$ w.r.t \mathbf{g}_r into an equivalent minimization problem, called *controlled approximation*; (ii) Establish an upper-bound of the controlled approximation objective such that its minimizer is analytic. This derivation is based on an important inequality: Poincaré inequality, which upper bounds the variances of a function by its gradient magnitude. Therefore, we need **Assumptions 7-8** (Appendix B) to make sure this inequality is valid. We name the resulting \mathbf{g}_r that minimizes the upper bound as *active slices*. All proofs can be found in appendix F.

4.1. Controlled Approximation

To start with, we need an upper bound for $S_{\mathbf{g}_r}$ so that we can transform the maximization of $S_{\mathbf{g}_r}$ into the minimization of their gap. Hence, we propose a generalization of SD (Eq.2) called *projected Stein discrepancy* (PSD):

$$\text{PSD}(q, p; O_r) = \sum_{\mathbf{r} \in O_r} \sup_{f_r \in \mathcal{F}_q} \mathbb{E}_q [s_p^T(\mathbf{x}) f_r(\mathbf{x}) + \mathbf{r}^T \nabla_{\mathbf{x}} f_r(\mathbf{x})] \quad (9)$$

where $f_r : \mathcal{X} \subseteq \mathbb{R}^D \rightarrow \mathbb{R}$. SD is a special case of PSD by setting O_r as identity matrix \mathbf{I} . In proposition 4 of appendix F.1, we show that if \mathcal{F}_q contains all bounded continuous functions, then the optimal test function in PSD is

$$f_r^*(\mathbf{x}) \propto (s_p^r(\mathbf{x}) - s_q^r(\mathbf{x})). \quad (10)$$

It can also be shown that PSD is equivalent to the *Fisher divergence*, which has been extensively used in training energy based models (Song et al., 2020; Song & Ermon, 2019) and fitting kernel exponential families (Sriperumbudur et al., 2017; Sutherland et al., 2018; Wenliang et al., 2019).

We now prove that PSD upper-bounds $S_{\mathbf{g}_r}$, with the gap as the expected square error between their optimal test functions f_r^* and h_{r, \mathbf{g}_r}^* (Proposition 1). Since PSD is constant w.r.t. \mathbf{g}_r , maximization of $S_{\mathbf{g}_r}$ is equivalent to a minimization task, called *controlled approximation*.

Theorem 3 (Controlled Approximation). *Assume assumptions 1-4 (density regularity), and the coefficient for the optimal test functions to be 1 w.l.o.g., then $\text{PSD} \geq S_{\mathbf{g}_r}$ and*

$$\text{PSD} - S_{\mathbf{g}_r} = \sum_{\mathbf{r} \in O_r} \mathbb{E}_q [(f_r^*(\mathbf{x}) - h_{r, \mathbf{g}_r}^*(\mathbf{x}^T \mathbf{g}_r))^2], \quad (11)$$

with f_r^* and h_{r, \mathbf{g}_r}^* are optimal test functions for PSD and $S_{\mathbf{g}_r}$ defined in Eq.10 and Eq.8 respectively.

Intuitively, minimizing the above gap can be regarded as a function approximation problem, where we want to approximate a multivariate function $f_r^* : \mathbb{R}^D \rightarrow \mathbb{R}$ by a univariate function $h_{r, \mathbf{g}_r}^* : \mathbb{R} \rightarrow \mathbb{R}$ with optimal parameters \mathbf{g}_r .

4.2. Upper-bounding the error

Solving the controlled approximation task directly may be difficult in practice. Instead, we propose an upper-bound of the approximation error, such that this upper-bound’s minimizer \mathbf{g}_r is analytic. The inspiration comes from the *active subspace method* for dimensionality reduction (Constantine et al., 2014; Zahm et al., 2020), therefore we name the corresponding minimizers as *active slices*.

Theorem 4 (Error upper-bound and active slices \mathbf{g}_r). *Assume assumptions 2, 4 (density regularity) and 7-8 (Poincaré inequality conditions), we can upper bound the inner part of the controlled approximation error (Eq.11) by*

$$\mathbb{E}_q \left[(f_r^*(\mathbf{x}) - h_{r, \mathbf{g}_r}^*(\mathbf{x}^T \mathbf{g}_r))^2 \right] \leq C_{\text{sup}} \text{tr} \left(\mathbf{G}_{r \setminus d} \mathbf{H}_r \mathbf{G}_{r \setminus d}^T \right), \quad (12)$$

$$\mathbf{H}_r = \int q(\mathbf{x}) \nabla_{\mathbf{x}} f_r^*(\mathbf{x}) \nabla_{\mathbf{x}} f_r^*(\mathbf{x})^T d\mathbf{x}. \quad (13)$$

Here C_{sup} is the Poincaré constant defined in assumption 8 and $\mathbf{G}_{r \setminus d} \in \mathbb{R}^{(D-1) \times D}$ is an arbitrary orthogonal matrix

\mathbf{G}_r excluding the d^{th} row \mathbf{g}_r . The orthogonal matrix has the form $\mathbf{G}_r = [\mathbf{a}_1, \dots, \mathbf{a}_D]^T$ where $\mathbf{a}_i \in \mathbb{S}^{D-1}$ and $\mathbf{a}_d = \mathbf{g}_r$.

The above upper-bound is minimized when the row space of $\mathbf{G}_{r \setminus d}$ is the span of the first $D - 1$ eigenvectors of \mathbf{H}_r (arranging eigenvalues in ascending order). One possible choice for active slice \mathbf{g}_r is \mathbf{v}_D , where $(\lambda_i, \mathbf{v}_i)$ is the eigenpair of \mathbf{H}_r and $\lambda_1 \leq \lambda_2 \leq \dots \leq \lambda_D$.

Intuitively, the active slices $\mathbf{g}_r = \mathbf{v}_D$ are the directions where the test function f_r^* varies the most. Indeed, we have $\mathbf{v}_D^T \mathbf{H}_r \mathbf{v}_D = \mathbb{E}_q[|\nabla_{\mathbf{x}} f_r^*(\mathbf{x})^T \mathbf{v}_D|^2] = \lambda_D$, where the eigenvalue λ_D measures the averaged gradient variation in the direction defined by \mathbf{v}_D .

5. Active slice direction r

The dependence of active slice \mathbf{g}_r on r motivate us to consider the possible choices of r . Although finite random slices r are sufficient for obtaining a valid discrepancy, in practice using sub-optimal r can result in weak discriminative power and poor active slices \mathbf{g}_r . We address this issue by proposing an efficient algorithm to search for good r . Again all the proofs can be found in appendix G.

5.1. PSD Maximization for searching r

Directly optimizing S_{r, g_r} w.r.t. r is particularly difficult due to the alternated updates of r and \mathbf{g}_r . To simplify the analysis, we start from the task of finding a single direction r . Our key idea to sidestep such alternation is based on the intuition that S_{r, g_r} with active slices \mathbf{g}_r should well approximate PSD_r (PSD with given r) from theorem 4. The independence of PSD_r to \mathbf{g}_r allows us to avoid the alternated update and the accurate approximation validates the direct usage of the resulting active slices in S_{r, g_r} . Indeed, we will prove that maximizing PSD_r is equivalent to maximizing a lower-bound for S_{r, g_r} .

Assume we have two slices r_1 and r_2 , with given $\mathbf{g}_{r_1}, \mathbf{g}_{r_2}$. Then finding good r_1 is equivalent to maximizing the difference $S_{r_1, g_{r_1}} - S_{r_2, g_{r_2}}$. The following proposition establishes a lower-bound for this difference.

Proposition 2 (Lower-bound for the S_{r, g_r} gap). *Assume the conditions in theorem 4 are satisfied, then for any slices r_1, r_2 and $\mathbf{g}_{r_1}, \mathbf{g}_{r_2}$, we have*

$$S_{r_1, g_{r_1}} - S_{r_2, g_{r_2}} \geq \text{PSD}_{r_1} - \text{PSD}_{r_2} - C_{\text{sup}} \Omega, \quad (14)$$

where C_{sup} is the Poincaré constant defined in assumption 8 and $\Omega = \sum_{i=1}^D \omega_i$ where $\{\omega_i\}_i^D$ is the eigenvalue of $\mathbb{E}_q[\nabla_{\mathbf{x}} \mathbf{f}^*(\mathbf{x}) \nabla_{\mathbf{x}} \mathbf{f}^*(\mathbf{x})^T]$, $\mathbf{f}^*(\mathbf{x}) = \mathbf{s}_p(\mathbf{x}) - \mathbf{s}_q(\mathbf{x})$.

Proposition 2 justifies the maximization of PSD_{r_1} w.r.t. r_1 as a valid surrogate. But more importantly, this alternative

objective admits an analytic maximizer of r , which is then used as the active slice direction:

Theorem 5 (Active slice r). *Assuming assumptions 1-4 (density regularity), then the maximum of the PSD $_r$ is achieved at $r^* = \mathbf{v}_{\max}$:*

$$\max_{r \in \mathbb{S}^{D-1}} \mathbb{E}_q [s_p^r(\mathbf{x}) f_r^*(\mathbf{x}) + r^T \nabla_{\mathbf{x}} f_r^*(\mathbf{x})] = \lambda_{\max}.$$

Here $(\lambda_{\max}, \mathbf{v}_{\max})$ is the largest eigenpair of the matrix $\mathbf{S} = \mathbb{E}_q [\mathbf{f}^*(\mathbf{x}) \mathbf{f}^*(\mathbf{x})^T]$

5.2. Constructing the orthogonal basis O_r

Under certain scenarios, e.g. model learning, we want to train the model to perform well in every directions instead of a particular one. Thus, using a good orthogonal basis is preferred over a single active slice r . Here gradient-based optimization is less suited as it breaks the orthogonality constraint. Also proposition 2 is less useful here as well, as PSD is invariant to the choice of O_r , i.e. $\text{PSD}(q, p; O_{r_1}) = \text{PSD}(q, p; O_{r_2})$ and $O_{r_1} \neq O_{r_2}$.

Inspired by the analysis of single active r , we propose to use the eigendecomposition of \mathbf{S} to obtain a good orthogonal basis O_r . Theoretically, this operation also corresponds to a greedy algorithm, where in step i it searches for the optimal direction r_i that is orthogonal to $\{r_{<i}\}$ and maximizes PSD_{r_i} (see Corollary 6.2 in appendix G.3). Although there is no guarantee for finding the *optimal* O_r due to its myopic behavior, in practice this greedy algorithm at least finds some good directions with high discriminative power (eigenvectors with large eigenvalues).

6. Practical algorithm

The proposed active slice method is summarized in Algorithm 1, which requires the intractable score difference $s_p(\mathbf{x}) - s_q(\mathbf{x})$. Two types of approximations can be used. The first approach applies *gradient estimators* (GE) to estimate $s_q(\mathbf{x})$ from \mathbf{x} samples. We use the Stein gradient estimator (Li & Turner, 2017) for the GE approach, although other estimators (Sriperumbudur et al., 2017; Sutherland et al., 2018; Shi et al., 2018; Zhou et al., 2020) can also be employed. The second method directly estimates the score difference using a *kernel-smoothed estimator* (KE):

$$\begin{aligned} s_p(\mathbf{y}) - s_q(\mathbf{y}) &\approx \mathbb{E}_{\mathbf{x} \sim q} [(s_p(\mathbf{x}) - s_q(\mathbf{x})) k(\mathbf{x}, \mathbf{y})] \\ &= \mathbb{E}_{\mathbf{x} \sim q} [s_p(\mathbf{x}) k(\mathbf{x}, \mathbf{y}) + \nabla_{\mathbf{x}} k(\mathbf{x}, \mathbf{y})], \end{aligned} \quad (15)$$

where the second expression comes from integration by part, and it can be computed in practice. Figure 1 summarizes the relationships between different SSD discrepancies and highlights our contributions. For GOF test specifically, we also derive the asymptotic distribution and propose an practical GOF algorithm in appendix D.

Algorithm 1 Active slice algorithm

Input: Samples $\mathbf{x} \sim q$, density p , kernel $k : \mathcal{X} \times \mathcal{X} \rightarrow \mathbb{R}$, Gaussian noise γ , pruning factor m (optional)
Result: $\widetilde{O}_r, \mathbf{G}$
 Estimate $s_p(\mathbf{x}) - s_q(\mathbf{x})$ using KE or GE with kernel k and samples \mathbf{x} .
if Pruning **then**
 Top m eigenvectors of \mathbf{S} to form \widetilde{O}_r (Theorem 5)
else
 Getting all eigenvectors of \mathbf{S} to form \widetilde{O}_r
end if
 Add noise γ to \widetilde{O}_r , then normalize. (Section 3.1)
for $\mathbf{r} \in \widetilde{O}_r$ **do**
 \mathbf{g}_r is the top 1 eigenvector of \mathbf{H}_r (Theorem 4)
 Add noise γ to \mathbf{g}_r then normalize (Section 3.1)
 Concatenate \mathbf{g}_r to \mathbf{G}
end for
 Further optimize $\widetilde{O}_r, \mathbf{G}$ with $SKSD-g$ (SK_{g_r}) using gradient-based optimization (Optional)
Return: $\widetilde{O}_r, \mathbf{G}$

6.1. Computational cost

The overall complexity includes the cost for (1) finding active slices (algorithm 1) (2) applying the downstream test. For finding the active slices \mathbf{r} , one important fact is that we only need the m ($m \ll D$) most important \mathbf{r} (importance characterised by eigenvalues). Luckily, fast eigenvalue-decomposition algorithm, e.g. randomized SVD from Saibaba et al. (2021), requires $O(m)$ matrix-vector product. For \mathbf{g} , from algorithm 1, we only need to solve m eigenvalue-decomposition, each only cares about the most important eigenvector. Therefore, $O(m \times 1)$ matrix-vector product are needed. So the overall complexity for finding slices is $O(mD^2)$, where D^2 comes from matrix-vector product. For gradient-based optimization (GO), the complexity is $O(l(D^2 + C_{\text{grad}}))$ (l is optimization step and C_{grad} is the back-prop cost, D^2 comes from evaluating SK_{g_r} or SK_{r, g_r}). Our algorithm in general has lower training cost as $l \gg m$ and C_{grad} can be expensive. For (2), our method has $O(mD)$ cost compared to $O(D^2)$ for GO. As $m \ll D$, active slices have less complexity compared to pure GO based method proposed in Gong et al. (2021). For memory cost, our method costs $O(mD)$ to store \mathbf{r}, \mathbf{g} whereas GO uses $O(D^2)$. Overall, our method requires nearly an order of magnitude less complexity in terms of computation and memory consumption.

7. Experiments

GOF test aims to test the fitness of the model to the target data. The test procedure roughly proceeds as: (1) Define null hypothesis (model matches the data distribution) and

alternative hypothesis (model does not match the data distribution); (2) Compute test statistic (e.g. KSD) and threshold (e.g. bootstrap method); (3) Reject null hypothesis (statistic $>$ threshold) or not (statistic \leq threshold). Refer to appendix D for more details.

7.1. Benchmark GOF tests

We demonstrate the improved test power results (in terms of null rejection rates) and significant speed-ups of the proposed active slice algorithm on 3 benchmark tasks, which have been extensively used for measuring GOF test performances (Jitkrittum et al., 2017; Huggins & Mackey, 2018; Chwialkowski et al., 2016; Gong et al., 2021). Here the test statistic is based on $SKSD-g$ (SK_{g_r}) with fixed basis $O_r = \mathbf{I}$. Two practical approaches are considered for computing the active slice \mathbf{g}_r : (i) gradient estimation with the Stein gradient estimator ($SKSD-g+GE$), and (ii) gradient estimation with the kernel-smoothed estimator (KE), plus further gradient-based optimization ($SKSD-g+KE+GO$). For reference, we include a version of the algorithm with exact score difference ($SKSD-g+Ex$) as an ablation for the gradient estimation approaches.

In comparison, we include the following strong baselines: KSD with RBF kernel (Liu et al., 2016; Chwialkowski et al., 2016), maximum mean discrepancy (MMD, Gretton et al., 2012) with RBF kernel, random feature Stein discrepancy with L1-IMQ kernel (L1-IMQ, Huggins & Mackey, 2018), and the current state-of-the-art — $maxSKSD-g$ with random initialized \mathbf{g}_r followed by gradient optimization ($SKSD-g+GO$, Gong et al., 2021). For all methods requiring GO or active slices, we split the 1000 test samples from q into 800 test and 200 training data, where we run GO or active slice method on the training set.

The 3 GOF test benchmarks, with details in appendix H.1, are: (1) **Laplace**: $p(\mathbf{x}) = \mathcal{N}(0, \mathbf{I})$, $q(\mathbf{x}) = \prod_{d=1}^D \text{Lap}(x_d | 0, 1/\sqrt{2})$; (2) **Multivariate-t**: $p(\mathbf{x}) = \mathcal{N}(0, \frac{5}{3}\mathbf{I})$, $q(\mathbf{x})$ is a fully factorized multivariate-t with 5 degrees of freedom, 0 mean and scale 1; (3) **Diffusion**: $p(\mathbf{x}) = \mathcal{N}(0, \mathbf{I})$, $q(\mathbf{x}) = \mathcal{N}(\mathbf{0}, \Sigma_1)$ where in $q(\mathbf{x})$ the variance of 1st-dim is 0.3 and the rest is \mathbf{I} .

The upper panels in Figure 2 show the test power results as the dimensions D increase. As expected, KSD and MMD with RBF kernel suffer from the curse-of-dimensionality. $L1-IMQ$ performs relatively well in **Laplace** and **multivariate-t** but still fails in **diffusion**. For $SKSD$ based approaches, $SKSD-g+GO$ with 1000 training epochs still exhibits a decreasing test power in **Laplace** and **multivariate-t**. On the other hand, $SKSD-g+KE+GO$ with 50 training epochs has nearly optimal performance. $SKSD-g+Ex$ and $SKSD-g+GE$ achieve the true optimal rejection rate without any GO . Specifically, Table 2 shows that the active slice method achieves significant computational savings

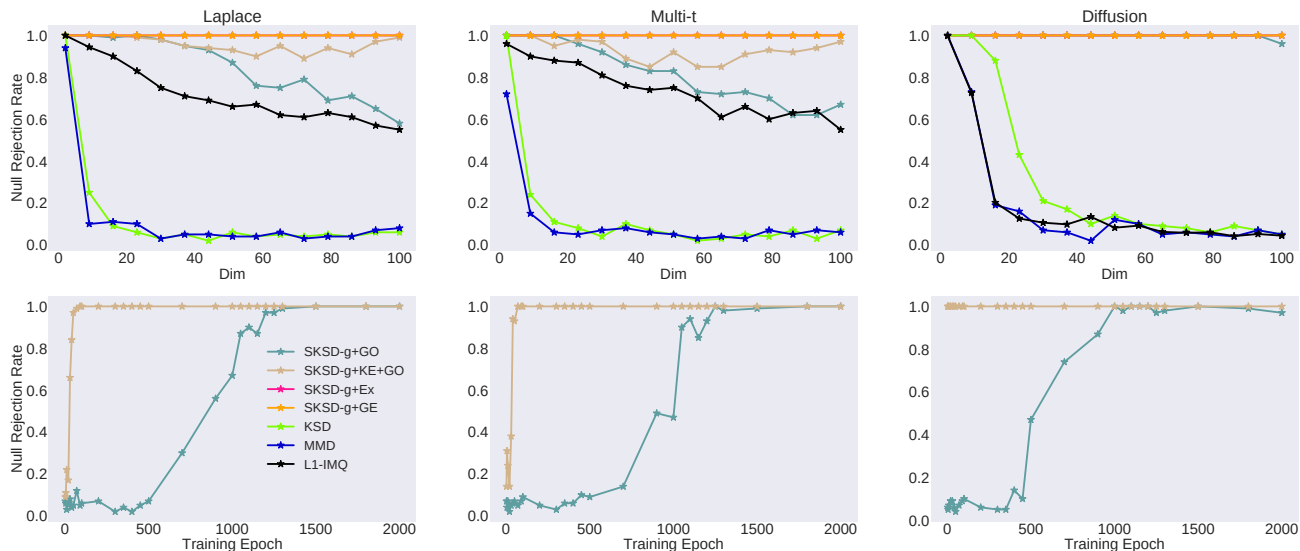


Figure 2. (**Upper panel**): The null rejection rate w.r.t. different dimensional benchmark problems. *SKSD-g+Ex* and *SKSD-g+GE* coincide at the optimal rejection rate (**Lower panel**): Null rejection rate with different number of gradient optimization epochs.

with **14x-80x** speed-up over *SKSD-g+GO*.

For approaches that require gradient optimization, the lower panels in Figure 2 show the test power as the number of training epochs increases. *SKSD-g+GO* with random slice initialization requires a huge number of gradient updates to obtain reasonable test power, and 1000 epochs achieves the best balance between run-time and performance. On the other hand, *SKSD-g+KE+GO* with active slice achieves significant speed-ups with near-optimal test power using around **50** epochs on **Laplace** and **Multivariate-t**. Remarkably, on **Diffusion** test, \mathbf{g}_r initialized by the active slices achieves near-optimal results already, so that the later gradient refinements are not required.

7.2. RBM GOF test

Following Gong et al. (2021), we conduct a more complex GOF test using restrict Boltzman machines (RBMs, (Hinton & Salakhutdinov, 2006; Welling et al.)). Here the p distribution is an RBM: $p(\mathbf{x}) = \frac{1}{Z} \exp(\mathbf{x}^\top \mathbf{B} \mathbf{h} + \mathbf{b}^\top \mathbf{x} + \mathbf{c}^\top \mathbf{x} - \frac{1}{2} \|\mathbf{x}\|^2)$, where $\mathbf{x} \in \mathbb{R}^D$ and $\mathbf{h} \in \{\pm 1\}^{d_h}$ denotes the hidden variables. The q distribution is also an RBM with the same \mathbf{b}, \mathbf{c} parameters as p but a different \mathbf{B} matrix perturbed by different levels of Gaussian noise. We use $D = 50$ and $d_h = 40$, and block Gibbs sampler with 2000 burn-in steps. The test statistics for all the approaches are computed on a test set containing 1000 samples from q .

The test statistic is constructed using *SKSD-rg* (SK_{rg_r}) with \mathbf{r}, \mathbf{g}_r obtained either by gradient-based optimization (*SKSD-rg+GO*) or the active slice algorithms (*+KE, +GE*

and *+Ex*) without the gradient refinements. Specifically, *SKSD-rg+GO* runs 50 training epochs with \mathbf{r} and \mathbf{g}_r initialized to \mathbf{I} . For the active slice methods, we also prune away most slices and only keep the top-3 most important \mathbf{r} slices.

The left panel of Figure 3 shows that *SKSD-rg+KE* achieves the best null rejection rates among all baselines, except for *SKSD-rg+Ex* whose performance is expected to upper-bound all other active slice methods. This shows the potential of our approach with an accurate score difference estimator. Although *SKSD-rg+GO* performs reasonably well, its run-time is **53x** longer than *SKSD-rg+KE* as shown in Table 4. Interestingly, *SKSD-rg+GE* performs worse than KSD due to the significant under-estimation of the magnitude of $s_q(\mathbf{x})$. Therefore, we omit this approach in the following ablation studies.

Ablation studies The first ablation study, with results shown in the middle panel in Figure 3, considers pruning the active slices at different pruning levels, where the horizontal axis indicates the number of \mathbf{r} slices used to construct the test statistic. We observe that the null rejection rates of active slice methods peak with pruning level 3, indicating their ability to select the most important directions. Their performances decrease when more \mathbf{r} are considered since, in practice, those less important directions introduce extra noise to the test statistic. On the other hand, *SKSD-rg+GO* shows no pruning abilities due to its sensitivity to slice initialization. Remarkably, the final performance of *SKSD-rg+GO* without pruning is still worse than *SKSD-rg+KE* with pruning, showing the importance of finding 'good' instead of many 'average-quality' directions. Another advantage of

Table 2. Test power for 100 dimensional benchmarks and time consumption. The run-time for SKSD-g+KE+GO include both the active slice computation and the later gradient-based refinement steps. NRR stands for null rejection rate.

Method	Laplace			Multi-t			Diffusion		
	NRR	sec/trial	Speed-up	NRR	sec/trial	Speed-up	NRR	sec/trial	Speed-up
SKSD-g+Ex	1	0.38	103x	1	0.49	90x	1	0.34	102x
SKSD-g+GO	0.58	39.39	1x	0.67	44.24	1x	0.96	34.73	1x
SKSD-g+KE+GO	0.99	2.72	14x	0.97	2.38	19x	1	0.43	81x
SKSD-g+GE	1	0.66	60x	1	0.67	66x	1	0.78	44x



Figure 3. (Left): The GOF test power of each method with different level of noise perturbations (Mid): The effect of different pruning level towards the test power (Right): The effect of gradient based optimization epoch to the test power. 3 and 50 indicates the pruning level. *KE+GO* or *Ex+GO* means active slices with further gradient refinement steps.

pruning is to reduce the computational and memory costs from $O(MD)$ to $O(mD)$, where m and M are the number of pruned r and slice initializations, respectively ($m \ll M$).

The second ablation study investigates the quality of the obtained slices either by gradient-based optimization or by the active slice approaches. Results are shown in the right panel of Figure 3, where the horizontal axis indicates the number of training epochs, and the numbers annotated in the legend (3 and 50) indicate the pruning. We observe that the null rejection rate of *SKSD-rg+KE+GO* starts to improve only after 100 epochs, meaning that short run of *GO* refinements are redundant due to the good quality of active slices. The performance decrease of *SKSD-rg+Ex+GO* is due to the over-fitting of *GO* to the training set. The null rejection rate of *SKSD-rg+GO* gradually increases with larger training epochs as expected. However, even after 100 epochs, the test power is still lower than active slices without any *GO*.

In appendix H.2, another ablation study also shows the advantages of good r compared to using random slices.

7.3. Model learning: ICA

We evaluate the performance of the active slice methods in model learning by training an independent component analysis (ICA) model, which has been extensively used to evaluate algorithms for training energy-based models (Gutmann & Hyvärinen, 2010; Hyvärinen & Dayan, 2005; Ceylan & Gutmann, 2018; Grathwohl et al., 2020). ICA follows a simple generative process: it first samples a D -

dimensional random variable z from a non-Gaussian p_z (we use multivariate-t), then transforms z to $x = \mathbf{W}z$ with a non-singular matrix $\mathbf{W} \in \mathbb{R}^{D \times D}$. The log-likelihood is $\log p(x) = \log p_z(\mathbf{W}^{-1}x) + C$ where C can be ignored if trained by minimizing Stein discrepancies. We follow Grathwohl et al. (2020); Gong et al. (2021) to sample 20000 training and 5000 test datapoints from a randomly initialized ICA model. The baselines considered include *KSD*, *SKSD-g+GO*, *SKSD-rg+GO* and the state-of-the-art learned Stein discrepancy (*LSD*) (Grathwohl et al., 2020), where the test function is parametrized by a neural network. For active slice approaches, one optimization epoch include the following two steps: (i) finding active slices for both orthogonal basis O_r and g_r at the beginning of the epoch, and (ii) refining the g_r directions and the \mathbf{W} parameters in an adversarial manner with O_r fixed. For *SKSD-g+GO*, we fix basis $O_r = \mathbf{I}$ and only update g_r with *GO*. We refer to appendix H.3 for details on the setup and training procedure. We see from Figure 4 that *SKSD-g+KE+GO* converges significantly faster at 150 dimensions than all baselines; moreover, it has much better NLL (Table 3). We argue this performance gain is due to the use of the better orthogonal basis O_r found by the greedy algorithm, showing the advantages of better O_r in model learning. On the other hand, the importance of orthogonality in O_r is indicated by the poor performance of *SKSD-rg+GO*, as gradient updates for r violate the orthogonality constraint. The goal of learning is to train the model to match the data distribution along every slicing direction, and the orthogonality constraint can help prevent the model from ignoring important slicing directions.

Table 3. The test NLL of different dimensional ICA model

Dimensions	SKSD-g+KE+GO	SKSD-g+Ex+GO	SKSD-g+GO	SKSD-rg+GO	LSD	KSD
10	7.93±0.31	7.95±0.31	8.06±0.33	10.03±0.61	7.42±0.31	7.82±0.31
80	7.88±0.77	15.17±0.97	19.03±1.06	62.53±0.92	6.26±1.49	80.75±1.22
100	6.93±1.36	21.50±1.41	22.22±1.08	75.28±1.63	17.55±1.60	110.78±1.19
150	11.67±2.46	27.37±3.04	21.63±3.27	107.25±1.93	32.15±3.75	180.47±1.91

Table 4. Test power and time consumption at 0.01 perturbation

	Test Power	Opt. Time	Speed-up
SKSD-rg+Ex	0.95	0.04s	254x
SKSD-rg+KE	0.67	0.19s	53x
SKSD-rg+GO	0.45	10.15s	1x

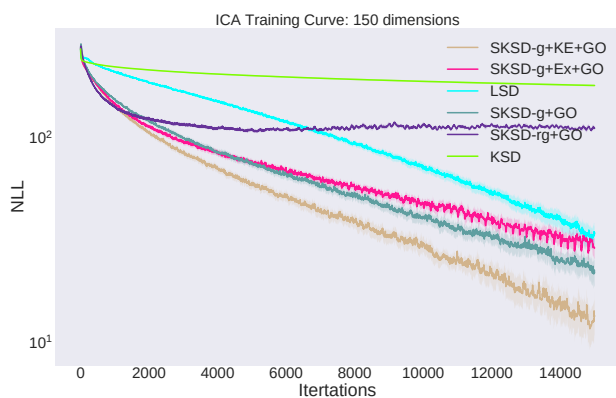


Figure 4. Training Curve of ICA model, where y-axis indicates the test NLL.

Interestingly, *SKSD-g+Ex+GO* performs worse than *+KE+GO*. We hypothesize that this is because the *+Ex+GO* approach often focuses on directions with large discriminative power but with less useful learning signal (see appendix H.3). *LSD* performs well in low dimensional problems. However, in high dimensional learning tasks it spends too much time on finding good test functions, which slows down the convergence significantly.

8. Related Work

Active subspace method (ASM): ASM is initially proposed as a dimensionality reduction method, which constructs a subspace with low-rank projectors (Constantine et al., 2014) according to the subspace Poincaré inequality. Zahm et al. (2020) showed promising results on the application of ASM to approximating multivariate functions with lower dimensional ones. However, they only considered the subspace Poincaré inequality under Gaussian measures, and a generalization to a broader family of family is proposed by Parente et al. (2020). Another closely related approach uses logarithmic Sobolev inequality in-

stead to construct the active subspace (Zahm et al., 2018), which can be interpreted as finding the optimal subspace to minimize a KL-divergence. It has shown successes in Bayesian inverse problems and particle inference (Chen et al., 2019). However, as the ASM method is based on the eigen-decomposition of the sensitivity matrix, there is a potential limitation when the sensitivity matrix is estimated by Monte-Carlo method. We prove this limitation in appendix I.

Sliced discrepancies: Existing examples of sliced discrepancies can be roughly divided into two groups. Most of them belong to the first group, and they use the slicing idea to improve computational efficiency. For example, sliced Wasserstein distance projects distributions onto one dimensional slices so that the corresponding distance has an analytic form (Kolouri et al., 2019; Deshpande et al., 2019). Sliced score matching uses Hutchinson’s trick to avoid the expensive computation of the Hessian matrix (Song et al., 2020). The second group focuses on the curse-of-dimensionality issue which remains to be addressed. To the best of our knowledge, existing integral probability metrics in this category include *SSD* (Gong et al., 2021) and *kernelized complete conditional Stein discrepancy* (KCC-SD, Singhal et al., 2019). The former is more general and requires less restrictive assumptions, while the latter requires samples from complete conditional distributions. Recent work has also investigated the statistical properties of sliced discrepancies (Nadjahi et al., 2020).

9. Conclusion

We have proposed the active slice method as a practical solution for searching good slices for *SKSD*. We first prove that the validity of the kernelized discrepancy only requires finite number of random slices instead of optimal ones, giving us huge freedom to select slice directions. Then by analyzing the approximation quality of *SSD* to *SKSD*, we proposed to find active slices by optimizing surrogate optimization tasks. Experiments on high-dimensional GOF tests and ICA training showed the active slice method performed the best across a number of competitive baselines in terms of both test performance and run-time. Future research directions include better score difference estimation methods, non-linear generalizations of slice projections, and the application of the active slice method to other discrepancies.

References

- Arcones, M. A. and Gine, E. On the bootstrap of u and v statistics. *The Annals of Statistics*, pp. 655–674, 1992.
- Ceylan, C. and Gutmann, M. U. Conditional noise-contrastive estimation of unnormalised models. In *International Conference on Machine Learning*, pp. 726–734. PMLR, 2018.
- Chen, P., Wu, K., Chen, J., O’Leary-Roseberry, T., and Ghattas, O. Projected stein variational newton: A fast and scalable bayesian inference method in high dimensions. *arXiv preprint arXiv:1901.08659*, 2019.
- Chwialkowski, K., Strathmann, H., and Gretton, A. A kernel test of goodness of fit. *JMLR: Workshop and Conference Proceedings*, 2016.
- Comon, P. Independent component analysis, a new concept? *Signal processing*, 36(3):287–314, 1994.
- Constantine, P. G., Dow, E., and Wang, Q. Active subspace methods in theory and practice: applications to kriging surfaces. *SIAM Journal on Scientific Computing*, 36(4): A1500–A1524, 2014.
- Deshpande, I., Hu, Y.-T., Sun, R., Pyrros, A., Siddiqui, N., Koyejo, S., Zhao, Z., Forsyth, D., and Schwing, A. G. Max-sliced wasserstein distance and its use for gans. In *Proceedings of the IEEE/CVF Conference on Computer Vision and Pattern Recognition*, pp. 10648–10656, 2019.
- Gong, W., Li, Y., and Hernández-Lobato, J. M. Sliced kernelized stein discrepancy. In *International Conference on Learning Representations*, 2021. URL <https://openreview.net/forum?id=t0TaKv0Gx6Z>.
- Gorham, J. and Mackey, L. Measuring sample quality with stein’s method. In *Advances in Neural Information Processing Systems*, pp. 226–234, 2015.
- Gorham, J. and Mackey, L. Measuring sample quality with kernels. In *International Conference on Machine Learning*, pp. 1292–1301. PMLR, 2017.
- Grathwohl, W., Wang, K.-C., Jacobsen, J.-H., Duvenaud, D., and Zemel, R. Cutting out the middle-man: Training and evaluating energy-based models without sampling. *arXiv preprint arXiv:2002.05616*, 2020.
- Gretton, A., Borgwardt, K. M., Rasch, M. J., Schölkopf, B., and Smola, A. A kernel two-sample test. *The Journal of Machine Learning Research*, 13(1):723–773, 2012.
- Gutmann, M. and Hyvärinen, A. Noise-contrastive estimation: A new estimation principle for unnormalized statistical models. In *Proceedings of the Thirteenth International Conference on Artificial Intelligence and Statistics*, pp. 297–304. *JMLR Workshop and Conference Proceedings*, 2010.
- Hinton, G. E. and Salakhutdinov, R. R. Reducing the dimensionality of data with neural networks. *science*, 313(5786):504–507, 2006.
- Hoeffding, W. A class of statistics with asymptotically normal distribution. In *Breakthroughs in statistics*, pp. 308–334. Springer, 1992.
- Hu, T., Chen, Z., Sun, H., Bai, J., Ye, M., and Cheng, G. Stein neural sampler. *arXiv preprint arXiv:1810.03545*, 2018.
- Huggins, J. and Mackey, L. Random feature stein discrepancies. In *Advances in Neural Information Processing Systems*, pp. 1899–1909, 2018.
- Huskova, M. and Janssen, P. Consistency of the generalized bootstrap for degenerate u -statistics. *The Annals of Statistics*, pp. 1811–1823, 1993.
- Hyvärinen, A. and Dayan, P. Estimation of non-normalized statistical models by score matching. *Journal of Machine Learning Research*, 6(4), 2005.
- Jitkrittum, W., Xu, W., Szabó, Z., Fukumizu, K., and Gretton, A. A linear-time kernel goodness-of-fit test. In *Advances in Neural Information Processing Systems*, pp. 262–271, 2017.
- Kingma, D. P. and Ba, J. Adam: A method for stochastic optimization. *arXiv preprint arXiv:1412.6980*, 2014.
- Kolouri, S., Nadjahi, K., Simsekli, U., Badeau, R., and Rohde, G. K. Generalized sliced wasserstein distances. *arXiv preprint arXiv:1902.00434*, 2019.
- Li, Y. and Turner, R. E. Gradient estimators for implicit models. *arXiv preprint arXiv:1705.07107*, 2017.
- Liu, Q. and Wang, D. Stein variational gradient descent: A general purpose bayesian inference algorithm. *arXiv preprint arXiv:1608.04471*, 2016.
- Liu, Q., Lee, J., and Jordan, M. A kernelized stein discrepancy for goodness-of-fit tests. In *International conference on machine learning*, pp. 276–284, 2016.
- Mityagin, B. The zero set of a real analytic function. *arXiv preprint arXiv:1512.07276*, 2015.
- Nadjahi, K., Durmus, A., Chizat, L., Kolouri, S., Shahrampour, S., and Şimşekli, U. Statistical and topological properties of sliced probability divergences. *arXiv preprint arXiv:2003.05783*, 2020.

- Parente, M. T., Wallin, J., Wohlmuth, B., et al. Generalized bounds for active subspaces. *Electronic Journal of Statistics*, 14(1):917–943, 2020.
- Pu, Y., Gan, Z., Henao, R., Li, C., Han, S., and Carin, L. Vae learning via stein variational gradient descent. *arXiv preprint arXiv:1704.05155*, 2017.
- Saibaba, A. K., Hart, J., and van Bloemen Waanders, B. Randomized algorithms for generalized singular value decomposition with application to sensitivity analysis. *Numerical Linear Algebra with Applications*, pp. e2364, 2021.
- Sameh, A. and Tong, Z. The trace minimization method for the symmetric generalized eigenvalue problem. *Journal of computational and applied mathematics*, 123(1-2):155–175, 2000.
- Serfling, R. J. *Approximation theorems of mathematical statistics*, volume 162. John Wiley & Sons, 2009.
- Shi, J., Sun, S., and Zhu, J. A spectral approach to gradient estimation for implicit distributions. *arXiv preprint arXiv:1806.02925*, 2018.
- Singhal, R., Han, X., Lahlou, S., and Ranganath, R. Kernelized complete conditional stein discrepancy. *arXiv preprint arXiv:1904.04478*, 2019.
- Song, Y. and Ermon, S. Generative modeling by estimating gradients of the data distribution. In *Advances in Neural Information Processing Systems*, pp. 11918–11930, 2019.
- Song, Y., Garg, S., Shi, J., and Ermon, S. Sliced score matching: A scalable approach to density and score estimation. In *Uncertainty in Artificial Intelligence*, pp. 574–584. PMLR, 2020.
- Sriperumbudur, B., Fukumizu, K., Gretton, A., Hyvärinen, A., and Kumar, R. Density estimation in infinite dimensional exponential families. *The Journal of Machine Learning Research*, 18(1):1830–1888, 2017.
- Sriperumbudur, B. K., Fukumizu, K., and Lanckriet, G. R. Universality, characteristic kernels and rkhs embedding of measures. *Journal of Machine Learning Research*, 12(7), 2011.
- Sutherland, D., Strathmann, H., Arbel, M., and Gretton, A. Efficient and principled score estimation with nyström kernel exponential families. In *International Conference on Artificial Intelligence and Statistics*, pp. 652–660. PMLR, 2018.
- Welling, M., Rosen-Zvi, M., and Hinton, G. E. Exponential family harmoniums with an application to information retrieval. Citeseer.
- Wenliang, L., Sutherland, D., Strathmann, H., and Gretton, A. Learning deep kernels for exponential family densities. In *International Conference on Machine Learning*, pp. 6737–6746. PMLR, 2019.
- Yu, Y., Wang, T., and Samworth, R. J. A useful variant of the davis–kahan theorem for statisticians. *Biometrika*, 102(2):315–323, 2015.
- Zahm, O., Cui, T., Law, K., Spantini, A., and Marzouk, Y. Certified dimension reduction in nonlinear bayesian inverse problems. *arXiv preprint arXiv:1807.03712*, 2018.
- Zahm, O., Constantine, P. G., Prieur, C., and Marzouk, Y. M. Gradient-based dimension reduction of multivariate vector-valued functions. *SIAM Journal on Scientific Computing*, 42(1):A534–A558, 2020.
- Zhou, Y., Shi, J., and Zhu, J. Nonparametric score estimators. *arXiv preprint arXiv:2005.10099*, 2020.

A. Terms and Notations

For the clarity of the paper, we give a summary of the commonly used notations in the main text and proof.

Symbols:

$\mathbf{s}_p(\mathbf{x})$	$\nabla_{\mathbf{x}} \log p(\mathbf{x})$
$\mathbf{s}_p^r(\mathbf{x})$	Projected score function $\nabla_{\mathbf{x}} \log p(\mathbf{x})^T \mathbf{r}$
\mathcal{X}	A subset of \mathbb{R}^D
\mathcal{K}	A subset of \mathbb{R} .
k_{r,g_r}	kernel function $k : \mathcal{K} \times \mathcal{K} \rightarrow \mathcal{R}$
\mathcal{H}_{r,g_r}	Induced RKHS by the kernel k_{r,g_r} .
$\ \cdot\ _{\mathcal{H}_{r,g_r}}$	RKHS norm of \mathcal{H}_{r,g_r}
\mathbf{g}_r	Input projection direction (e.g. $\mathbf{x}^T \mathbf{g}_r$) for corresponding r .
\mathbf{r}	Score projection direction (e.g. $\mathbf{s}_p^r(\mathbf{x}) = \mathbf{s}_p(\mathbf{x})^T \mathbf{r}$)
$S_{\max_{g_r}}$	$maxSSD-g$ (Eq.4).
S_{g_r}	$SSD-g$, i.e. $S_{\max_{g_r}}$ (Eq.4) without \sup_{g_r} . But with summation of O_r .
S_{r,g_r}	$SSD-rg$, i.e. $S_{\max_{g_r}}$ (Eq.4) without \sup_{g_r} and summation of O_r . Instead, we use specific r .
$SK_{\max_{g_r}}$	$maxSKSD-g$. The kernelized version of $S_{\max_{g_r}}$
SK_{g_r}	$SKSD-g$. The kernelized version of S_{g_r}
SK_{r,g_r}	$SKSD-rg$. The kernelized version of S_{r,g_r}
PSD	Projected Stein discrepancy (Eq.9)
PSD $_r$	Projected Stein discrepancy (Eq.9) without summation O_r and use specific r instead.
f_r^*	Optimal test function for PSD. $f_r^*(\mathbf{x}) \propto \mathbf{s}_p^r(\mathbf{x}) - \mathbf{s}_q^r(\mathbf{x})$
h_{r,g_r}^*	Optimal test function for S_{g_r} with specific r and \mathbf{g}_r , defined in Eq.8.
*	This indicates the optimal test function (e.g. f_r^*)
C_{\sup}	Supremum of Poincaré constant defined in assumption 6.

A.1. "Sub-optimal" variants of SSD

For the ease of the analysis, we want to define the notations without the sup operator over the slice directions \mathbf{r} , \mathbf{g}_r . Here, we define $SSD-g$ (S_{g_r}) as the $maxSSD-g$ ($S_{\max_{g_r}}$ in Eq.4) without the \sup_{g_r} .

$$S_{g_r} = \sum_{\mathbf{r} \in O_r} \sup_{h_{r,g_r} \in \mathcal{F}_q} \mathbb{E}_q[s_p^r(\mathbf{x}) h_{r,g_r}(\mathbf{x}^T \mathbf{g}_r) + \mathbf{r}^T \mathbf{g}_r \nabla_{\mathbf{x}^T \mathbf{g}_r} h_{r,g_r}(\mathbf{x}^T \mathbf{g}_r)] \quad (16)$$

Similarly, we define $SSD-rg$ (S_{r,g_r}) as $maxSSD-rg$ ($S_{\max_{r,g_r}}$ in Eq.37) without \sup_{r,g_r} :

$$S_{r,g_r} = \sup_{h_{r,g_r} \in \mathcal{F}_q} \mathbb{E}_q[s_p^r(\mathbf{x}) h_{r,g_r}(\mathbf{x}^T \mathbf{g}_r) + \mathbf{r}^T \mathbf{g}_r \nabla_{\mathbf{x}^T \mathbf{g}_r} h_{r,g_r}(\mathbf{x}^T \mathbf{g}_r)] \quad (17)$$

As for each of the above "optimal" discrepancies, it has the corresponding kernelized version. Therefore, we need to define their "un-optimal" version as well. We define $SKSD-g$ (SK_{g_r}) as $maxSKSD-g$ ($SK_{\max_{g_r}}$ in Eq.6) as

$$SK_{g_r} = \sum_{\mathbf{r} \in O_r} \|\mathbb{E}_q[\xi_{p,r,g_r}(\mathbf{x})]\|_{\mathcal{H}_{r,g_r}}^2, \quad (18)$$

Similarly, we define $SKSD-rg$ (SK_{r,g_r}) as $maxSKSD-rg$ ($SK_{\max_{r,g_r}}$ in Eq.41) as

$$SK_{r,g_r} = \|\mathbb{E}_q[\xi_{p,r,g_r}(\mathbf{x})]\|_{\mathcal{H}_{r,g_r}}^2 \quad (19)$$

B. Assumptions and Definitions

Definition B.1 (Inner product in Hilbert space). *We denote the algebraic space \mathbb{R}^D refers to a parameter space of dimension D . The Borel sets of \mathbb{R}^D is denoted as $\mathcal{B}(\mathbb{R}^D)$, and we let $\mu(x)$ be a probability measure on \mathbf{x} . We define*

$$\mathcal{H}_\mu = L^2(\mathbb{R}^D, \mathcal{B}(\mathbb{R}^D), \mu) \quad (20)$$

as the Hilbert space which contains all the measurable functions $f : \mathbb{R}^D \rightarrow \mathbb{R}$, such that $\|f\|_{\mathcal{H}_\mu} \leq \infty$, where we define inner product $\langle \cdot, \cdot \rangle_{\mathcal{H}_\mu}$ to be

$$\langle f, g \rangle_{\mathcal{H}_\mu} = \int f(\mathbf{x})g(\mathbf{x})d\mu(\mathbf{x}) \quad (21)$$

for all $f, g \in \mathcal{H}_\mu$

Definition B.2. (*Stein Class (Liu et al., 2016)*) *Assume distribution q has continuous and differentiable density $q(\mathbf{x})$. A function f defined on the domain $\mathcal{X} \subseteq \mathbb{R}^D$, $f : \mathcal{X} \rightarrow \mathbb{R}$ is in the **Stein class of q** if f is smooth and satisfies*

$$\int_{\mathcal{X}} \nabla_{\mathbf{x}}(f(\mathbf{x})q(\mathbf{x}))d\mathbf{x} = 0 \quad (22)$$

We call a function $f(\mathbf{x}) \in \mathcal{F}_q$ if f belongs to the Stein class of q . We say vector-valued function $\mathbf{f}(\mathbf{x}) : \mathcal{X} \subseteq \mathbb{R}^D \rightarrow \mathbb{R}^m \in \mathcal{F}_q$ if each component of \mathbf{f} belongs to the Stein class of q .

Definition B.3 (Stein Identity). *Assume q is a smooth density satisfied assumption 1, then we have*

$$\mathbb{E}_q[s_q(\mathbf{x})f(\mathbf{x})^T + \nabla f(\mathbf{x})] = 0 \quad (23)$$

for any functions $f : \mathcal{X} \subseteq \mathbb{R}^D \rightarrow \mathbb{R}^D$ in Stein class of q .

We can easily see that the above holds true for $\mathcal{X} = \mathbb{R}^D$ if

$$\lim_{\|\mathbf{x}\| \rightarrow \infty} q(\mathbf{x})f(\mathbf{x}) = 0 \quad (24)$$

Assumption 1 (Properties of densities) Assume the two probability distributions p, q has continuous differentiable density $p(\mathbf{x}), q(\mathbf{x})$ supported on $\mathcal{X} \subseteq \mathbb{R}^D$, such that the induced set $\mathcal{K} = \{y \in \mathbb{R} | y = \mathbf{x}^T \mathbf{g}, \|\mathbf{g}\|^2 = 1, \mathbf{x} \in \mathcal{X}\}$ is *locally compact Hausdorff* (LCH) for all possible $\mathbf{g} \in \mathbb{S}^{D-1}$. If $\mathcal{X} = \mathbb{R}^D$, then the density q satisfies: $\lim_{\|\mathbf{x}\| \rightarrow \infty} q(\mathbf{x}) = 0$. If $\mathcal{X} \subset \mathbb{R}^D$ is compact, then $q(\mathbf{x}) = 0$ at boundary $\partial \mathcal{X}$.

Assumption 2 (Regularity of score functions) Denote the score function of $p(\mathbf{x})$ as $\mathbf{s}_p(\mathbf{x}) = \nabla_{\mathbf{x}} \log p(\mathbf{x}) \in \mathbb{R}^D$ and score function of $q(\mathbf{x})$ accordingly. Assume the score functions are bounded continuous differentiable functions and satisfying

$$\begin{aligned} \int_{\mathcal{X}} q(\mathbf{x}) |(\mathbf{s}_p(\mathbf{x}) - \mathbf{s}_q(\mathbf{x}))^T \mathbf{r}| d\mathbf{x} < \infty \\ \int_{\mathcal{X}} q(\mathbf{x}) \|(\mathbf{s}_p(\mathbf{x}) - \mathbf{s}_q(\mathbf{x}))^T \mathbf{r}\|^2 d\mathbf{x} < \infty \end{aligned} \quad (25)$$

for all \mathbf{r} where $\mathbf{r} \in \mathbb{S}^{D-1}$.

Assumption 3 (Test functions) Assume the test function $h_{r, g_r} : \mathcal{K} \subseteq \mathbb{R} \rightarrow \mathbb{R}$ is smooth and belongs to the Stein class of q . Specifically, if with assumption 1, we only requires h_{r, g_r} to be a bounded continuous function. Similarly, we assume this also holds for PSD (eq.9) test function $f_r(\mathbf{x})$.

Assumption 4 (Bounded Conditional Expectation) Define

$$h_{r, g_r}^*(y_d) = \mathbb{E}_{q_{G_r}(\mathbf{y}_{-d}|y_d)}[(s_p^T(\mathbf{G}_r^{-1} \mathbf{y}) - s_q^T(\mathbf{G}_r^{-1} \mathbf{y}))] \quad (26)$$

as in proposition 1. We assume h_{r, g_r}^* is uniformly bounded for all possible $\mathbf{g}_r \in \mathbb{S}^{D-1}$.

Assumption 5 (universal kernel): We assume the kernel $k_{r, g} : \mathcal{K} \times \mathcal{K} \rightarrow \mathbb{R}$ is bounded and c_0 -universal.

Assumption 6 (Real analytic translation invariant kernel): We assume the kernel is translation invariant $k(x, y) = \phi(x - y) : \mathcal{K} \rightarrow \mathbb{R}$ and ϕ is a real analytic function. Additionally, we assume if $k(cx, cy) = k'(x, y)$ for a constant $c > 0$ where k' is also a c_0 -universal kernel. For example, *radial basis kernel function* (RBF) and *inverse multiquadric* (IMQ) kernel satisfy these assumptions.

Assumption 7 (Log-concave probabilities) Assume a probability distribution q with density function such that $q(\mathbf{x}) = \exp(-V(\mathbf{x}))$, where $V(\mathbf{x})$ is a convex function.

Assumption 8 (Existence of supremum of Poincaré constant). For the Poincaré constant defined in lemma 5, the essential supremum exists $C_{ess, \mathbf{G}} = \text{ess sup}_{y_d} C_{y_d} < \infty$ and also the $C_{sup} = \sup_{\mathbf{G}} C_{ess, \mathbf{G}} < \infty$ exists over all possible orthogonal matrix \mathbf{G} .

C. Detailed Background

C.1. Stein Discrepancy

Assume we have two differentiable probability density functions $q(\mathbf{x})$ and $p(\mathbf{x})$ where $\mathbf{x} \in \mathcal{X} \subset \mathbb{R}^D$. We further define a test function $\mathbf{f} : \mathcal{X} \rightarrow \mathbb{R}^D$ and a suitable test function family \mathcal{F}_q called *Stein's class of q* . Recall the Stein operator (Eq.1) is defined as

$$\mathcal{A}_p \mathbf{f}(\mathbf{x}) = \mathbf{s}_p(\mathbf{x})^T \mathbf{f}(\mathbf{x}) + \nabla_{\mathbf{x}}^T \mathbf{f}(\mathbf{x}) \quad (27)$$

The function family \mathcal{F}_q is defined as

$$\mathcal{F}_q = \{\mathbf{f} : \mathcal{X} \rightarrow \mathbb{R}^D \mid \mathbb{E}_q[\mathcal{A}_q \mathbf{f}] = 0\} \quad (28)$$

This function space can be quite general. For example, if $\mathcal{X} = \mathbb{R}^D$, we only require \mathbf{f} to be differentiable and vanishing at infinity. With all the notations, *Stein discrepancy* is defined as follows:

$$D_{SD}(q, p) = \sup_{\mathbf{f} \in \mathcal{F}_q} \mathbb{E}_q[\mathcal{A}_p \mathbf{f}(\mathbf{x})] \quad (29)$$

which can be proved to be a valid discrepancy (Gorham & Mackey, 2017). Stein discrepancy has been shown to be closely related to *Fisher discrepancy* defined as

$$D_F(q, p) = \mathbb{E}_q \|\mathbf{s}_p(\mathbf{x}) - \mathbf{s}_q(\mathbf{x})\|_2^2 \quad (30)$$

Indeed, Hu et al. (2018) shows that the optimal test function for *Stein discrepancy* has the form $\mathbf{f}^*(\mathbf{x}) \propto \mathbf{s}_p(\mathbf{x}) - \mathbf{s}_q(\mathbf{x})$. By substitution, we can show *Stein discrepancy* is equivalent to *Fisher divergence* up to a multiplicative constant.

Unfortunately, the score difference $\mathbf{s}_p(\mathbf{x}) - \mathbf{s}_q(\mathbf{x})$ may be intractable in practice, making SD intractable as a consequence. Thus, Liu et al. (2016); Chwialkowski et al. (2016) propose an variant of SD by restricting \mathcal{F}_q to be a unit ball inside an RKHS \mathcal{H}_k induced by a c_0 -universal kernel $k : \mathcal{X} \times \mathcal{X} \rightarrow \mathbb{R}$. By using the reproducing properties, they propose *kernelized Stein discrepancy* as

$$\begin{aligned} D^2(q, p) &= \|\mathbb{E}_q[\mathbf{s}_p(\mathbf{x})k(\mathbf{x}, \cdot) + \nabla_{\mathbf{x}} k(\mathbf{x}, \cdot)]\|_{\mathcal{H}_k}^2 \\ &= \mathbb{E}_{\mathbf{x}, \mathbf{x}' \sim q}[u_p(\mathbf{x}, \mathbf{x}')] \end{aligned} \quad (31)$$

where $u_p(\mathbf{x}, \mathbf{x}')$ is

$$\begin{aligned} u_p(\mathbf{x}, \mathbf{x}') &= \mathbf{s}_p(\mathbf{x})^T k(\mathbf{x}, \mathbf{x}') \mathbf{s}_p(\mathbf{x}') + \mathbf{s}_p(\mathbf{x})^T \nabla_{\mathbf{x}'} k(\mathbf{x}, \mathbf{x}') \\ &+ \mathbf{s}_p(\mathbf{x}')^T \nabla_{\mathbf{x}} k(\mathbf{x}, \mathbf{x}') + \nabla_{\mathbf{x}, \mathbf{x}'}^2 k(\mathbf{x}, \mathbf{x}') \end{aligned} \quad (32)$$

and \mathbf{x}, \mathbf{x}' are i.i.d. samples from q .

Due to its tractability, it has been extensively used in statistical test e.g. GOF test Liu et al. (2016); Chwialkowski et al. (2016); Huggins & Mackey (2018); Jitkrittum et al. (2017). However, recent work demonstrate KSD suffers from the curse-of-dimensionality problem Gong et al. (2021); Huggins & Mackey (2018); Chwialkowski et al. (2016). One potential fix is to use another variant called *sliced kernelized Stein discrepancy*.

C.2. Sliced Kernelized Stein Discrepancy

In this section, we give a more detailed introduction to sliced kernelized Stein discrepancy (SKSD). Recall the definition of Stein discrepancy:

$$D_{SD}(q, p) = \sup_{\mathbf{f} \in \mathcal{F}_q} \mathbb{E}_q[s_p^T(\mathbf{x})\mathbf{f}(\mathbf{x}) + \nabla_{\mathbf{x}}^T \mathbf{f}(\mathbf{x})] \quad (33)$$

In the original paper of (Gong et al., 2021), they argue that the curse of dimensionality comes from two sources: (i) the high dimensionality of the score function $s_p : \mathcal{X} \subseteq \mathbb{R}^D \rightarrow \mathbb{R}^D$ and (ii) the test function input $\mathbf{x} \in \mathcal{X} \subseteq \mathbb{R}^D$. Therefore, authors proposed two slice directions \mathbf{r}, \mathbf{g} to project s_p and \mathbf{x} respectively. However, this projection is equivalent to throwing away most of the information possessed by s_p and \mathbf{x} . To tackle this problem, authors proposed the first member of the SSD family by considering over all possible directions of \mathbf{r} and \mathbf{g} (a distribution over $\mathbf{r} \sim p_r, \mathbf{g} \sim p_g$), called *integrated sliced Stein discrepancy*:

$$S(q, p) = \mathbb{E}_{p_r, p_g} \left[\sup_{h_{r,g} \in \mathcal{F}_q} \mathbb{E}_q[s_p^T(\mathbf{x})h_{r,g}(\mathbf{x}^T \mathbf{g}) + \mathbf{r}^T \mathbf{g} \nabla_{\mathbf{x}^T \mathbf{g}} h_{r,g}(\mathbf{x}^T \mathbf{g})] \right] \quad (34)$$

where $h_{r,g}$ is the test function. Although it is theoretically valid (Theorem 1 in (Gong et al., 2021)), its practical usage is limited by the intractability of the integral over p_r, p_g and the optimal test function $h_{r,g}$. Surprisingly, authors show that the integral over \mathbf{r}, \mathbf{g} is not necessary for discrepancy validity. They achieved this in two steps.

The first step is to replace the expectation w.r.t. \mathbf{r} by a finite summation over orthogonal basis. The author showed that this is a valid discrepancy, called *orthogonal sliced Stein discrepancy* defined as

$$S_O(q, p) = \sum_{\mathbf{r} \in O_r} \mathbb{E}_{p_g} \left[\sup_{h_{r,g} \in \mathcal{F}_q} \mathbb{E}_q[s_p^T(\mathbf{x})h_{r,g}(\mathbf{x}^T \mathbf{g}) + \mathbf{r}^T \mathbf{g} \nabla_{\mathbf{x}^T \mathbf{g}} h_{r,g}(\mathbf{x}^T \mathbf{g})] \right] \quad (35)$$

where O_r is an orthogonal basis (e.g. one-hot vectors). The next step is to get rid of the expectation w.r.t. \mathbf{g} by a supremum operator. This is called *maxSSD-g*, which is defined as Eq.4 in the main text. For a quick recall, we include *maxSSD-g* in here:

$$S_{\max_{g_r}}(q, p) = \sum_{\mathbf{r} \in O_r} \sup_{\substack{h_{r,g_r} \in \mathcal{F}_q \\ \mathbf{g}_r \in \mathbb{S}^{D-1}}} \mathbb{E}_q[s_p^T(\mathbf{x})h_{r,g_r}(\mathbf{x}^T \mathbf{g}_r) + \mathbf{r}^T \mathbf{g}_r \nabla_{\mathbf{x}^T \mathbf{g}_r} h_{r,g_r}(\mathbf{x}^T \mathbf{g}_r)] \quad (36)$$

Further, one can also use single optimal direction \mathbf{r} to replace the summation over the orthogonal basis O_r , resulting in *maxSSD-rg* ($S_{\max_{r,g_r}}$):

$$S_{\max_{r,g_r}}(q, p) = \sup_{h_{r,g} \in \mathcal{F}_q, \mathbf{g}_r, \mathbf{r} \in \mathbb{S}^{D-1}} \mathbb{E}_q [s_p^r(\mathbf{x})h_{r,g_r}(\mathbf{x}^T \mathbf{g}_r) + \mathbf{r}^T \mathbf{g}_r \nabla_{\mathbf{x}^T \mathbf{g}_r} h_{r,g_r}(\mathbf{x}^T \mathbf{g}_r)] \quad (37)$$

Similar to KSD, authors addressed tractability issue of the optimal h_{r,g_r} by restricting the \mathcal{F}_q to be a one-dimensional RKHS induced by a c_0 -universal kernel $k_{r,g} : \mathcal{K} \times \mathcal{K} \rightarrow \mathbb{R}$ where $\mathcal{K} \subseteq \mathbb{R}$. Thus, for each member of the above SSD family, we have a corresponding kernelized version. They are called *integrated sliced kernelized Stein discrepancy*, *orthogonal SKSD*, and *max sliced kernelized Stein discrepancy* (including *maxSKSD-g* and *maxSKSD-rg*). In practice, *maxSKSD-g* or *maxSKSD-rg* is often preferred over the others due to its computational tractability, where their optimal slices for \mathbf{r} and \mathbf{g}_r are obtained by gradient-based optimization.

By reproducing properties of RKHS, one can define $\xi_{p,r,g_r}(\mathbf{x}, \cdot)$ as in Eq.5, and further define $\mu_{p,r,g_r} = \langle \xi_{p,r,g_r}(\mathbf{x}, \cdot), \xi_{p,r,g_r}(\mathbf{y}, \cdot) \rangle_{\mathcal{H}_{r,g_r}}$

$$\begin{aligned} \mu_{p,r,g_r}(\mathbf{x}, \mathbf{y}) &= s_p^r(\mathbf{x})k_{r,g_r}(\mathbf{x}^T \mathbf{g}_r, \mathbf{y}^T \mathbf{g}_r)s_p^r(\mathbf{y}) \\ &\quad + \mathbf{r}^T \mathbf{g}_r s_p^r(\mathbf{y}) \nabla_{\mathbf{x}^T \mathbf{g}_r} k_{r,g_r}(\mathbf{x}^T \mathbf{g}_r, \mathbf{y}^T \mathbf{g}_r) \\ &\quad + \mathbf{r}^T \mathbf{g}_r s_p^r(\mathbf{x}) \nabla_{\mathbf{y}^T \mathbf{g}_r} k_{r,g_r}(\mathbf{x}^T \mathbf{g}_r, \mathbf{y}^T \mathbf{g}_r) \\ &\quad + (\mathbf{r}^T \mathbf{g}_r)^2 \nabla_{\mathbf{x}^T \mathbf{g}_r, \mathbf{y}^T \mathbf{g}_r}^2 k_{r,g_r}(\mathbf{x}^T \mathbf{g}_r, \mathbf{y}^T \mathbf{g}_r). \end{aligned} \quad (38)$$

Then, by simple algebra, one can show that given \mathbf{r}, \mathbf{g}_r , the optimality w.r.t. test functions can be computed analytically:

$$\begin{aligned} D_{r,g_r}^2(q, p) &= \left(\sup_{\substack{h_{r,g_r} \in \mathcal{H}_{r,g_r} \\ \|h_{r,g_r}\|_{\mathcal{H}_{r,g_r}} \leq 1}} \mathbb{E}_q[s_p^r(\mathbf{x})h_{r,g_r}(\mathbf{x}^T \mathbf{g}_r) + \mathbf{r}^T \mathbf{g}_r \nabla_{\mathbf{x}^T \mathbf{g}_r} h_{r,g_r}(\mathbf{x}^T \mathbf{g}_r)] \right)^2 \\ &= \|\mathbb{E}_q[\xi_{p,r,g_r}(\mathbf{x})]\|_{\mathcal{H}_{r,g_r}}^2 = \mathbb{E}_q(\mathbf{x} | \mathbf{x}') [\mu_{p,r,g_r}(\mathbf{x}, \mathbf{x}')]. \end{aligned} \quad (39)$$

where \mathcal{H}_{r,g_r} is the RKHS induced by the kernel k_{r,g_r} . Therefore, the *maxSSD-g* and *maxSSD-rg* can be computed as

$$SK_{\max_{g_r}}(q, p) = \sum_{\mathbf{r} \in O_r} \sup_{\mathbf{g}_r \in \mathbb{S}^{D-1}} D_{r,g_r}^2(q, p) \quad (40)$$

and

$$SK_{\max_{r,g_r}}(q, p) = \sup_{\substack{\mathbf{g}_r \in \mathbb{S}^{D-1} \\ \mathbf{r} \in \mathbb{S}^{D-1}}} D_{r,g_r}^2(q, p) \quad (41)$$

D. Goodness-of-fit test

In this section, we give an introduction to the GOF test. To be general, we focus on the $SKSD$ -rg ($SK_{rg_r} = \|\mathbb{E}_q[\xi_{p,r,g_r}(\mathbf{x})]\|_{\mathcal{H}_{rg_r}}^2$) as other related discrepancy can be easily derived from it. Assuming we have active slices \mathbf{r} and \mathbf{g}_r from algorithm 1. Thus, we can estimate SK_{rg_r} using the minimum variance U-statistics (Hoeffding, 1992; Serfling, 2009):

$$\widehat{SK}_{rg_r}(q, p) = \frac{1}{N(N-1)} \sum_{1 \leq i \neq j \leq N} \mu_{p,r,g_r}(\mathbf{x}_i, \mathbf{x}_j). \quad (42)$$

where $\mu_{\mathbf{x}, \mathbf{y}}$ is defined in Eq.38 which satisfies $\mathbb{E}_{q(\mathbf{x})q(\mathbf{x}')}[\mu_{p,r,g_r}(\mathbf{x}, \mathbf{x}')] = \|\mathbb{E}_q[\xi_{p,r,g_r}(\mathbf{x})]\|_{\mathcal{H}_{rg_r}}^2$, and \mathbf{x}, \mathbf{x}' are i.i.d. samples from q . With the help of the U-statistics, we characterize its asymptotic distribution.

Theorem 6. *Assume the conditions in theorem 1 are satisfied, we have the following:*

1. If $q \neq p$, then \widehat{SK}_{rg_r} is asymptotically normal. Particularly,

$$\sqrt{N}(\widehat{SK}_{rg_r} - SK_{rg_r}) \xrightarrow{d} \mathcal{N}(0, \sigma_h^2) \quad (43)$$

where $\sigma_h^2 = \text{var}_{\mathbf{x} \sim q}(\mathbb{E}_{\mathbf{x}' \sim q}[\mu_{p,r,g_r}(\mathbf{x}, \mathbf{x}')])$ and $\sigma_h \neq 0$

2. If $q = p$, we have a degenerated U-statistics with $\sigma_h = 0$ and

$$N\widehat{SK}_{rg_r} \xrightarrow{d} \sum_{j=1}^{\infty} c_j(Z_j^2 - 1) \quad (44)$$

where $\{Z_j\}$ are i.i.d standard Gaussian variables, and $\{c_j\}$ are the eigenvalues of the kernel $\mu_{p,r,g_r}(\mathbf{x}, \mathbf{x}')$ under $q(\mathbf{x})$. In other words, they are the solutions of $c_j \phi_j(\mathbf{x}) = \int_{\mathbf{x}'} \mu_{p,r,g_r}(\mathbf{x}, \mathbf{x}') \phi_j(\mathbf{x}') q(\mathbf{x}') d\mathbf{x}'$.

Proof. As the \widehat{SK}_{rg_r} is the second order U-statistic of SK_{rg_r} , thus, we can directly use the results from section 5.5.1 and 5.5.2 in (Serfling, 2009). \square

The above theorem indicates a well-defined asymptotic distribution for SK_{rg_r} , which allows us to use the following bootstrap method to estimate the rejection threshold (Huskova & Janssen, 1993; Arcones & Gine, 1992; Liu et al., 2016). The bootstrap samples can be computed as

$$\widehat{SK}_m^* = \sum_{1 \leq i \neq j \leq N} (w_i^m - \frac{1}{N})(w_j^m - \frac{1}{N}) \mu_{p,r,g_r}(\mathbf{x}_i, \mathbf{x}_j) \quad (45)$$

where $(w_1^m, \dots, w_N^m)_{m=1}^M$ are random weights drawn from multinomial distributions $\text{Multi}(N, \frac{1}{N}, \dots, \frac{1}{N})$. Now, we give the detailed algorithm for GOF test.

Algorithm 2 GOF test with active slices

Input: Samples $\mathbf{x} \sim q$, density p , kernel k_{rg_r} , active slices \mathbf{r}, \mathbf{g}_r , significance level α , and bootstrap sample size M .

Hypothesis: $H_0: p = q$ v.s. $H_1: p \neq q$

Computing U-statistics \widehat{SK}_{rg_r} using Eq.42

Generate M bootstrap samples $\{\widehat{SK}_m^*\}_{m=1}^M$ using Eq.45

Reject null hypothesis H_0 if the proportion of $\widehat{SK}_m^* > \widehat{SK}_{rg_r}$ is less than α

E. Relaxing constraints for kernelized SSD family

E.1. Validity w.r.t \mathbf{r}, \mathbf{g}_r

The key to this proof is to prove the real analyticity of SK_{g_r} (or S_{rg_r}) to slices \mathbf{r} and \mathbf{g}_r . Therefore, let's first give a definition of multivariate real analytic function.

Definition E.1 (Real analytic function). *A function $f: \mathcal{U} \rightarrow \mathbb{R}$ is real analytic if for each $\mathbf{c} \in \mathcal{U}$, there is a power series as in the form*

$$f(\mathbf{x}) = \sum_{\kappa \in \mathbb{N}_0^n} \alpha_{\kappa} (\mathbf{x} - \mathbf{c})^{\kappa}$$

for some choice of $(\alpha_{\kappa})_{\kappa \in \mathbb{N}_0^n} \subset \mathbb{R}$ and all \mathbf{x} in a neighbourhood of \mathbf{c} , and this power series converges absolutely. Namely,

$$\sum_{\kappa \in \mathbb{N}_0^n} |\alpha_{\kappa}| |\mathbf{x} - \mathbf{c}|^{\kappa} < \infty$$

where $\mathbb{N}_0 = \{0, 1, \dots\}$ denotes non-negative integers, $\kappa = (\kappa_1, \dots, \kappa_n)$ are called multiindex, and we define $\mathbf{x}^{\kappa} = x_1^{\kappa_1} \dots x_n^{\kappa_n}$.

Now, we introduce a useful lemma showing that composition of real analytic function is also real analytic.

Lemma 1 (Composition of real analytic function). *Let $\mathcal{U} \subset \mathbb{R}^n$ and $\mathcal{V} \subset \mathbb{R}^m$ be open, and let $\mathbf{f}: \mathcal{U} \rightarrow \mathcal{V}$ and $\mathbf{g}: \mathcal{V} \rightarrow \mathbb{R}^p$ be real analytic. Then $\mathbf{g} \circ \mathbf{f}: \mathcal{U} \rightarrow \mathbb{R}^p$ is real analytic.*

Especially, the real analyticity is not only preserved by function composition, it is also closed under most of the simple operations: addition, multiplication, division (assuming denominator is non-zero), etc. Now we can prove the main proposition to show that the $SKSD$ -rg (SK_{rg_r}) is real analytic w.r.t both \mathbf{g}_r and \mathbf{r} . In the following, we assume the $\mathbf{r}, \mathbf{g}_r \in \mathbb{R}^D$.

Proposition 3 (*SKSD-g is real analytic*). *Assume assumption 1-4 (density regularity), 5-6 (kernel richness and real analyticity) are satisfied, further we let $\mathbf{g}_r \in \mathbb{R}^D$, then SKSD-g (SK_{g_r}) is real analytic w.r.t \mathbf{g}_r and SK_{r, g_r} is real analytic to both $\mathbf{r} \in \mathbb{R}^D$ and \mathbf{g}_r .*

Proof. First, let's focus on the real analyticity w.r.t. \mathbf{g}_r . We re-write the SKSD-g as the following:

$$\begin{aligned} SK_{g_r} &= \sum_{\mathbf{r} \in O_r} \|\xi_{p,r,g_r}(\mathbf{x})\|_{\mathcal{H}_{r,g_r}}^2 \\ &= \sum_{\mathbf{r} \in O_r} \langle \mathbb{E}_q[(s_p^r(\mathbf{x}) - s_q^r(\mathbf{x})) \underbrace{k_{r,g_r}(\mathbf{x}^T \mathbf{g}_r, \cdot)}_{f_r^*(\mathbf{x})}], \\ &\quad \mathbb{E}_q[(s_p^r(\mathbf{x}) - s_q^r(\mathbf{x})) k_{r,g_r}(\mathbf{x}^T \mathbf{g}_r, \cdot)] \rangle_{\mathcal{H}_{r,g_r}} \\ &= \sum_{\mathbf{r} \in O_r} \mathbb{E}_{\mathbf{x}, \mathbf{x}'} [f_r^*(\mathbf{x}) k_{r,g_r}(\mathbf{x}^T \mathbf{g}_r, \mathbf{x}'^T \mathbf{g}_r) f_r^*(\mathbf{x}')] \end{aligned}$$

The second equality is from the definition of RKHS norm $\|\cdot\|_{\mathcal{H}_{r,g_r}}$ and Stein identity. We can observe that \mathbf{g}_r appears inside the kernel k_{r,g_r} in the form of $\mathbf{x}^T \mathbf{g}_r$. So in order to use the function composition lemma (lemma 1), we need to first show that for any given \mathbf{x} , $\mathbf{x}^T \mathbf{g}_r$ is real analytic. By definition of real analytic function, we need a center point $c \in \mathbb{R}^D$, and \mathbf{g}_r in the neighborhood of c (i.e. $|\mathbf{g}_r - c| < R_c$). Then, we define the power series as

$$h_x(\mathbf{g}_r) = \sum_{\kappa_1=0}^{\infty} \dots \sum_{\kappa_D=0}^{\infty} \frac{(g_{r1} - c_1)^{\kappa_1} \dots (g_{rD} - c_D)^{\kappa_D}}{\kappa_1! \dots \kappa_D!} \alpha_{\{\kappa_i\}_i^D} \mathbf{g}_r.$$

with the following coefficient

$$\begin{cases} \alpha_{\{\kappa_i\}_i^D} = 0 & \text{if } \sum_i \kappa_i > 1 \\ \alpha_{\{\kappa_i\}_i^D} = x_i & \text{if } \kappa_i = 1, \sum_i \kappa_i = 1 \\ \alpha_{\{\kappa_i\}_i^D} = \mathbf{c}^T \mathbf{x} & \text{if } \sum_i \kappa_i = 0 \end{cases}$$

Then, by substitution, we have

$$h_x(\mathbf{g}) = \sum_{d=1}^D (g_d - c_d) x_d + \mathbf{c}^T \mathbf{x} \quad (46)$$

$$= \mathbf{x}^T \mathbf{g} \quad (47)$$

which converges with radius of convergence $R_c = \infty$. From assumption 6, we know the kernel $k_{r,g_r}(\mathbf{x}^T \mathbf{g}_r, \mathbf{x}'^T \mathbf{g}_r) = \phi((\mathbf{x} - \mathbf{x}')^T \mathbf{g}_r)$ is translation invariant and real analytic. Thus, from lemma 1, we know $k_{r,g_r}(\mathbf{x}^T \mathbf{g}_r, \mathbf{x}'^T \mathbf{g}_r)$ is real analytic to \mathbf{g}_r with radius of convergence R_k (R_k is determined by the form of the kernel function). This means we can use a power series to represents this kernel w.r.t. \mathbf{g}_r inside some neighborhood define around center point. Specifically, for a central point $c \in \mathbb{R}^D$ and any \mathbf{g}_r satisfying $|\mathbf{g}_r - c| < R_k$, we have

$$k_{r,g_r}(\mathbf{x}^T \mathbf{g}_r, \mathbf{x}'^T \mathbf{g}_r) = \sum_{\kappa \in \mathbb{N}_0^D} \alpha_{\kappa}(\mathbf{x}, \mathbf{x}') (\mathbf{g}_r - c)^{\kappa}$$

where this series converges absolutely. We substitute it into SK_{g_r}

$$\begin{aligned} SK_{g_r} &= \sum_{\mathbf{r} \in O_r} \mathbb{E}_{\mathbf{x}, \mathbf{x}'} [f_r^*(\mathbf{x}) k_{r,g_r}(\mathbf{x}^T \mathbf{g}_r, \mathbf{x}'^T \mathbf{g}_r) f_r^*(\mathbf{x}')] \\ &= \sum_{\mathbf{r} \in O_r} \mathbb{E}_{\mathbf{x}, \mathbf{x}'} [f_r^*(\mathbf{x}) \sum_{\kappa \in \mathbb{N}_0^D} \alpha_{\kappa}(\mathbf{x}, \mathbf{x}') (\mathbf{g}_r - c)^{\kappa} f_r^*(\mathbf{x}')] \\ &= \sum_{\mathbf{r} \in O_r} \sum_{\kappa \in \mathbb{N}_0^D} \mathbb{E}_{\mathbf{x}, \mathbf{x}'} [\alpha_{\kappa}(\mathbf{x}, \mathbf{x}') f_r^*(\mathbf{x}) f_r^*(\mathbf{x}')] (\mathbf{g}_r - c)^{\kappa} \end{aligned}$$

which also converges absolutely with radius of convergence R_k . The third equality is from the Fubini's theorem. The conditions of Fubini's theorem can be verified by fact that f_r^* is square integrable (assumption 2), and the power series of k_{r,g_r} converges absolutely. Thus, by definition of real analytic function, SKSD-g is real analytic w.r.t each \mathbf{g}_r . This also implies SKSD-rg (SK_{r,g_r}) is real analytic w.r.t. \mathbf{g}_r (because SK_{r,g_r} is just SK_{g_r} without summation over O_r).

For the real analyticity w.r.t \mathbf{r} , the proof is almost the same. The inner product $s_p^r(\mathbf{x}) - s_q^r(\mathbf{x})$ is real analytic w.r.t \mathbf{r} obviously for given \mathbf{x} . We also use the fact that real analyticity is preserved under multiplication of two real analytic functions. In addition, note that $k_{r,g_r}(\mathbf{x}^T \mathbf{g}_r, \mathbf{x}'^T \mathbf{g}_r)$ act as a constant w.r.t. \mathbf{r} , we can directly apply the Fubini's theorem again to form a power series w.r.t. \mathbf{r} with absolute convergence. Thus, SK_{r,g_r} is real analytic w.r.t. \mathbf{r} for any \mathbf{g}_r . Thus, SK_{r,g_r} is real analytic to both \mathbf{r} and \mathbf{g}_r . \square

Next, we introduce an important property of real analytic function:

Lemma 2 (Zero Set Theorem (Mityagin, 2015)). *Let $f(x)$ be a real analytic function on (a connected open domain \mathcal{U} of) \mathbb{R}^d . If f is not identically 0, then its zero set*

$$S(f) := \{\mathbf{x} \in \mathcal{U} | f(\mathbf{x}) = 0\}$$

has a measure 0, i.e. $mes_d S(f) = 0$

With the help from the zero-set theorem, we can prove the validity of SK_{g_r} (or SK_{r,g_r}) with finite random slices \mathbf{g}_r (and \mathbf{r}).

Proof of theorem 1

Proof. We first deal with the validity of \mathbf{g}_r with fixed orthogonal basis O_r . It is trivial that when $p = q$, $SK_{g_r} = 0$ identically. Now, assume $p \neq q$, then, from the theorem 3 in (Gong et al., 2021), the orthogonal SKSD (Eq.48) is a valid discrepancy. Namely, we have

$$\sum_{\mathbf{r} \in O_r} \int q_{g_r}(\mathbf{g}_r) \|\mathbb{E}_q[\xi_{p,r,g_r}(\mathbf{x})]\|_{\mathcal{H}_{r,g_r}}^2 > 0 \quad (48)$$

We should note that the distribution q_{g_r} is originally defined on \mathbb{S}^{D-1} . But, we can easily generalize it to larger spaces.

As for $\mathbf{g}_r \in \mathbb{R}^D$, we can always write $\mathbf{g}_r = c\mathbf{g}'_r$, where $\mathbf{g}'_r \in \mathbb{S}^{D-1}$, and $c \geq 0$. As the domain for \mathbf{g}_r is \mathbb{R}^D , the \mathbf{g}_r can represent all possible directions. Thus, we can follow the same proof logic as theorem 3 in (Gong et al., 2021) to show the corresponding discrepancy is greater than 0 when $p \neq q$.

Therefore, Eq.48 represents there exists a $\mathbf{r} \in O_r$ such that $\|\mathbb{E}_q[\xi_{p,r,g_r}(\mathbf{x})]\|_{\mathcal{H}_{r,g_r}}^2 > 0$ for a set of \mathbf{g}_r with non-zero measure. Namely, $\|\mathbb{E}_q[\xi_{p,r,g_r}(\mathbf{x})]\|_{\mathcal{H}_{r,g_r}}^2$ is not 0 identically. Thus, from the proposition 3 and lemma 2, the set of \mathbf{g}_r that make $\|\mathbb{E}_q[\xi_{p,r,g_r}(\mathbf{x})]\|_{\mathcal{H}_{r,g_r}}^2 = 0$ has a 0 measure. Then, if \mathbf{g}_r is sampled from some distribution η_g with density supported on \mathbb{R}^D (e.g. Gaussian distribution), we have

$$SK_{g_r} = \sum_{\mathbf{r} \in O_r} \|\mathbb{E}_q[\xi_{p,r,g_r}(\mathbf{x})]\|_{\mathcal{H}_{r,g_r}}^2 > 0$$

almost surely.

Now, we show that SK_{r,g_r} is also a valid discrepancy with $\mathbf{r} \sim \eta_r$. First, due to the validity of *integrated SKSD*, we have

$$\int q_r(\mathbf{r}) \int q_{g_r}(\mathbf{g}_r) \|\mathbb{E}_q[\xi_{p,r,g_r}(\mathbf{x})]\|_{\mathcal{H}_{r,g_r}}^2 d\mathbf{g}_r d\mathbf{r} > 0 \quad (49)$$

Due to the real analyticity of SK_{r,g_r} ($\|\mathbb{E}_q[\xi_{p,r,g_r}(\mathbf{x})]\|_{\mathcal{H}_{r,g_r}}^2$) w.r.t \mathbf{r} , we can easily show that

$$\int q_{g_r}(\mathbf{g}_r) \|\mathbb{E}_q[\xi_{p,r,g_r}(\mathbf{x})]\|_{\mathcal{H}_{r,g_r}}^2 d\mathbf{g}_r$$

is real analytic to \mathbf{r} and it is not 0 identically. Thus, by lemma 2, for $\mathbf{r} \sim \eta_r$, we have

$$\int q_{g_r}(\mathbf{g}_r) \|\mathbb{E}_q[\xi_{p,r,g_r}(\mathbf{x})]\|_{\mathcal{H}_{r,g_r}}^2 d\mathbf{g}_r > 0$$

Namely, $\|\mathbb{E}_q[\xi_{p,r,g_r}(\mathbf{x})]\|_{\mathcal{H}_{r,g_r}}^2 > 0$ for a set of \mathbf{g}_r with non-zero measure. In the beginning of the proof, we show that this set of \mathbf{g}_r is almost everywhere in \mathbb{R}^D due to its real analyticity. Namely, $\|\mathbb{E}_q[\xi_{p,r,g_r}(\mathbf{x})]\|_{\mathcal{H}_{r,g_r}}^2 > 0$ for $\mathbf{r} \sim \eta_r$ and $\mathbf{g}_r \sim \eta_g$ if $p \neq q$. Thus, we can conclude that for $SK_{r,g_r} = 0$ if and only if $p = q$ almost surely for $\mathbf{r} \sim \eta_r$ and $\mathbf{g}_r \sim \eta_g$. \square

Corollary 6.1 (Normalizing \mathbf{g}_r). *Assume the conditions in theorem 1 are satisfied, then the following operations do not violate the validity of SKSD-rg SK_{r,g_r} . (1) For $\mathbf{g}'_r, \mathbf{r}' \in \mathbb{S}^{D-1}$, we define $\mathbf{g}_r = \mathbf{g}'_r + \gamma_g$ and $\mathbf{r} = \mathbf{r}' + \gamma_r$, where γ_r, γ_g are the noise from Gaussian distribution. (2) Define $\tilde{\mathbf{g}}_r = c_g \times \mathbf{g}_r$ and $\tilde{\mathbf{r}} = c_r \times \mathbf{r}$, where $\tilde{\mathbf{g}}_r, \tilde{\mathbf{r}}$ are unit vectors and $c_r, c_g > 0$. The resulting active slices $\tilde{\mathbf{r}}$ and $\tilde{\mathbf{g}}_r$ do not violate the validity of SK_{r,g_r} .*

Proof. From the theorem 1 with \mathbf{g}_r, \mathbf{r} , when $p \neq q$, we

have

$$\begin{aligned} SK_{r,g_r} &= \|\mathbb{E}_q[\xi_{p,r,g_r}(\mathbf{x})]\|_{\mathcal{H}_{r,g_r}}^2 \\ &= \mathbb{E}_{\mathbf{x}, \mathbf{x}'} [f_r^*(\mathbf{x}) k_{r,g_r}(\mathbf{x}^T \mathbf{g}_r, \mathbf{x}'^T \mathbf{g}_r) f_r^*(\mathbf{x}')] \\ &= \mathbb{E}_{\mathbf{x}, \mathbf{x}'} [c_r^2 f_{\tilde{r}}^*(\mathbf{x}) k_{r,g_r}(c\mathbf{x}^T \tilde{\mathbf{g}}_r, c\mathbf{x}'^T \tilde{\mathbf{g}}_r) f_{\tilde{r}}^*(\mathbf{x}')] > 0 \end{aligned}$$

From the assumption 6 that $k_{r,g_r}(c\mathbf{x}^T \tilde{\mathbf{g}}_r, c\mathbf{x}'^T \tilde{\mathbf{g}}_r) = k'_{r,g_r}(\mathbf{x}^T \tilde{\mathbf{g}}_r, \mathbf{x}'^T \tilde{\mathbf{g}}_r)$. So this is equivalent to the *SKSD-rg* defined with a new c_0 -universal kernel k'_{r,g_r} and $\tilde{\mathbf{g}}_r, \tilde{\mathbf{r}} \in \mathbb{S}^{D-1}$. Thus, the corresponding *maxSKSD-rg* with $\tilde{\mathbf{g}}_r, \tilde{\mathbf{r}} \in \mathbb{S}^{D-1}$ is a valid discrepancy almost surely. \square

E.2. Relationship between SSD and SKSD

Proof of proposition 1

Proof. We consider the *SSD-rg* (S_{r,g_r}) without the optimal test function:

$$\mathbb{E}_q[s_p^T(\mathbf{x}) h_{r,g_r}(\mathbf{x}^T \mathbf{g}_r) + \mathbf{r}^T \mathbf{g}_r \nabla_{\mathbf{x}^T \mathbf{g}_r} h_{r,g_r}(\mathbf{x}^T \mathbf{g}_r)] \quad (50)$$

From the Stein identity (Eq.23), we can let $\mathbf{f}(\mathbf{x}) = [r_1 h_{r,g_r}(\mathbf{x}^T \mathbf{g}_r), r_2 h_{r,g_r}(\mathbf{x}^T \mathbf{g}_r), \dots, r_D h_{r,g_r}(\mathbf{x}^T \mathbf{g}_r)]^T$ and then take the trace. Thus, we have

$$\mathbb{E}_q[s_p^T(\mathbf{x}) h_{r,g_r}(\mathbf{x}^T \mathbf{g}_r)] = \mathbb{E}_q[\mathbf{r}^T \mathbf{g}_r \nabla_{\mathbf{x}^T \mathbf{g}_r} h_{r,g_r}(\mathbf{x}^T \mathbf{g}_r)]$$

Substitute it into Eq.50 and change the variable to $\mathbf{y} = \mathbf{G}_r \mathbf{x}$, we have

$$\begin{aligned} &\mathbb{E}_q[(s_p^r(\mathbf{x}) - s_q^r(\mathbf{x})) h_{r,g_r}(\mathbf{x}^T \mathbf{g}_r)] \\ &= \int q_{G_r}(y_d, \mathbf{y}_{-d}) \underbrace{(s_p^r(\mathbf{G}_r^{-1} \mathbf{y}) - s_q^r(\mathbf{G}_r^{-1} \mathbf{y}))}_{f_r^*(\mathbf{G}_r^{-1} \mathbf{y})} h_{r,g_r}(y_d) d\mathbf{y} \\ &= \int q_{G_r}(y_d) \underbrace{\int q_{G_r}(\mathbf{y}_{-d} | y_d) f_r^*(\mathbf{G}_r^{-1} \mathbf{y}) d\mathbf{y}_{-d}}_{h_{r,g_r}^*(y_d)} h_{r,g_r}(y_d) dy_d \\ &\leq \sqrt{\mathbb{E}_{q_{G_r}(y_d)} [h_{r,g_r}^*(y_d)^2]} \sqrt{\mathbb{E}_{q_{G_r}(y_d)} [h_{r,g_r}(y_d)^2]} \end{aligned}$$

where the last inequality is from Cauchy-Schwarz inequality, where the equality holds when

$$\begin{aligned} h_{r,g_r}(y_d) &\propto h_{r,g_r}^*(y_d) \\ &= \mathbb{E}_{q_{G_r}(\mathbf{y}_{-d} | y_d)} [(s_p^r(\mathbf{G}_r^{-1} \mathbf{y}) - s_q^r(\mathbf{G}_r^{-1} \mathbf{y}))] \end{aligned}$$

where $y_d = \mathbf{x}^T \mathbf{g}_r$. \square

Proof of theorem 2

Proof. Let's first re-write of $S_{r_{g_r}}$ and $SK_{r_{g_r}}$.

$$\begin{aligned} S_{r_{g_r}} &= \sup_{h_{r_{g_r}} \in \mathcal{F}_q} \mathbb{E}_q[(s_p^r(\mathbf{y}) - s_q^r(\mathbf{x}))h_{r_{g_r}}(\mathbf{x}^T \mathbf{g}_r)] \\ &= \mathbb{E}_{q_{G_r}(y_d)} \left[\underbrace{\int q_{G_r}(\mathbf{y}-d|y_d) (s_p^r(\mathbf{G}_r^{-1} \mathbf{y}) - s_q^r(\mathbf{G}_r^{-1} \mathbf{y})) d\mathbf{y}_{-d}}_{h_{r_{g_r}}^*(y_d)} \right] \\ &\quad \times h_{r_{g_r}}^*(y_d) \\ &= \mathbb{E}_{q_{G_r}(y_d)} [h_{r_{g_r}}^*(y_d)^2] \end{aligned}$$

where the second equality is from proposition 1.

$$SK_{r_{g_r}} = \langle \mathbb{E}_q[\xi_{p,r,g_r}(\mathbf{x})], \mathbb{E}_q[\xi_{p,r,g_r}(\mathbf{x})] \rangle_{\mathcal{H}_k}$$

where $\xi_{p,r,g_r}(\mathbf{x}, \cdot)$ is defined in Eq.5, and $\langle \cdot, \cdot \rangle_{\mathcal{H}_{r_{g_r}}}$ is the RKHS inner product induced by kernel $k_{r_{g_r}}$. By simple algebraic manipulation and Stein identity (Eq.23), we have

$$\begin{aligned} &\mathbb{E}_q[\xi_{p,r,g_r}(\mathbf{x}, \cdot)] \\ &= \mathbb{E}_q[(s_p^r(\mathbf{x}) - s_q^r(\mathbf{x}))k_{r_{g_r}}(\mathbf{x}^T \mathbf{g}_r, \cdot)] \\ &= \mathbb{E}_{q_{G_r}(y_d)} \left[\underbrace{\int q_{G_r}(\mathbf{y}-d|y_d) (s_p^r(\mathbf{G}_r^{-1} \mathbf{y}) - s_q^r(\mathbf{G}_r^{-1} \mathbf{y})) d\mathbf{y}_{-d}}_{h_{r_{g_r}}^*(y_d)} \right] \\ &\quad \times k_{r_{g_r}}(y_d, \cdot) \\ &= \mathbb{E}_{q_{G_r}(y_d)} [h_{r_{g_r}}^*(y_d)k_{r_{g_r}}(y_d, \cdot)] \end{aligned}$$

Thus, we have

$$\begin{aligned} &SK_{r_{g_r}} \\ &= \mathbb{E}_{y_d, y'_d \sim q_{G_r}(y_d)} [h_{r_{g_r}}^*(y_d)k_{r_{g_r}}(y_d, y'_d)h_{r_{g_r}}^*(y'_d)] \\ &\leq \sqrt{\mathbb{E}_{y_d, y'_d} [k_{r_{g_r}}(y_d, y'_d)^2]} \sqrt{\mathbb{E}_{y_d} [h_{r_{g_r}}^*(y_d)^2]} \sqrt{\mathbb{E}_{y'_d} [h_{r_{g_r}}^*(y'_d)^2]} \\ &= M S_{r_{g_r}}^* \end{aligned}$$

where constant M is from the bounded kernel assumption, and the inequality is from Cauchy-Schwarz inequality. Without the loss of generality, we can set $M = 1$. For other value of $M > 0$, one can always set the optimal test function ($h_{r_{g_r}}^*$) for SSD -rg with coefficient M . The the new SSD -g will be M multiplied by the original SSD -rg with $M = 1$.

Thus, SSD -rg is an upper bound for $SKSD$ -rg. From the assumption 1, we know that the induced set $\mathcal{K} = \{y \in \mathbb{R} | y = \mathbf{x}^T \mathbf{g}, ||g|| = 1, \mathbf{x} \in \mathcal{X}\}$ is LCH, and the kernel $k_{r_{g_r}} : \mathcal{K} \times \mathcal{K} \rightarrow \mathbb{R}$ is c_0 -universal. Then, from (Sriperumbudur et al., 2011), c_0 -universal implies L_p -universal. Namely, the induced RKHS $\mathcal{H}_{r_{g_r}}$ is dense in $L^p(\mathcal{K}; \mu)$ with all Borel probability measure μ w.r.t. p -norm, defined as

$$||f||_p = \left(\int |f(\mathbf{x})|^p d\mu(\mathbf{x}) \right)^{\frac{1}{p}}$$

Now, from the assumption 4, we know $h_{r_{g_r}}^*(y_d)$ is bounded for all possible \mathbf{g}_r , we have

$$\int q_{G_r}(y_d) |h_{r_{g_r}}^*(y_d)|^2 dy_d < \infty$$

This means $h_{r_{g_r}}^* \in L^2(\mathcal{K}, \mu_{G_r})$, where μ_{G_r} is the probability measure with density $q_{G_r}(y_d)$

From the L_p -universality, there exists a function $\widetilde{h_{r_{g_r}}^*} \in \mathcal{H}_{r_{g_r}}$, such that for any given $\epsilon > 0$,

$$||h_{r_{g_r}}^* - \widetilde{h_{r_{g_r}}^*}||_2 < \epsilon$$

Let's define $\widetilde{SK}_{r_{g_r}}$ is the $SKSD$ -rg with the specific kernelized test function $\widetilde{h_{r_{g_r}}^*}$, and from the optimality of $SKSD$ -rg, we have

$$SK_{r_{g_r}} \geq \widetilde{SK}_{r_{g_r}}$$

Therefore, we have

$$\begin{aligned} 0 &\leq S_{r_{g_r}} - SK_{r_{g_r}} \\ &\leq S_{r_{g_r}} - \widetilde{SK}_{r_{g_r}} \\ &= \mathbb{E}_q[(s_p^r(\mathbf{x}) - s_q^r(\mathbf{x})) (h_{r_{g_r}}^*(\mathbf{x}^T \mathbf{g}_r) - \widetilde{h_{r_{g_r}}^*}(\mathbf{x}^T \mathbf{g}_r))] \\ &\leq \underbrace{\sqrt{\mathbb{E}_q[(s_p^r(\mathbf{x}) - s_q^r(\mathbf{x}))^2]}}_{C_r} \\ &\quad \times \sqrt{\mathbb{E}_q[(h_{r_{g_r}}^*(\mathbf{x}^T \mathbf{g}_r) - \widetilde{h_{r_{g_r}}^*}(\mathbf{x}^T \mathbf{g}_r))^2]} \\ &= C_r \sqrt{\int q_{G_r}(y_d, \mathbf{y}_{-d}) (h_{r_{g_r}}^*(y_d) - \widetilde{h_{r_{g_r}}^*}(y_d))^2 d\mathbf{y}} \\ &= C_r ||h_{r_{g_r}}^* - \widetilde{h_{r_{g_r}}^*}||_2 < C_r \epsilon \end{aligned}$$

From assumption 2, we know $s_p^r(\mathbf{x}) - s_q^r(\mathbf{x})$ is square integrable for all possible \mathbf{r} . Therefore, let's define $C = \max_{\mathbf{r} \in \mathbb{S}^{D-1}} C_r$, then,

$$0 \leq S_{r_{g_r}} - SK_{r_{g_r}} < C \epsilon$$

□

F. Theory related to active slice g

F.1. Optimal test function for PSD

Proposition 4 (Optimality of PSD). *Assume the assumption 1 – 3 (density regularity) are satisfied, then the optimal test function for PSD given O_r is proportional to the projected score difference, i.e.*

$$f_r^*(\mathbf{x}) \propto (s_p^r(\mathbf{x}) - s_q^r(\mathbf{x})) \quad (51)$$

Thus,

$$PSD(q, p; O_r) = \sum_{\mathbf{r} \in O_r} \mathbb{E}_q[(s_p^r(\mathbf{x}) - s_q^r(\mathbf{x}))^2] \quad (52)$$

if the coefficient of f_r^* to be 1.

Proof. From the Stein identity (Eq.23), we can re-write the inner part of the supremum of Eq.9 as

$$\begin{aligned} &\mathbb{E}_q[s_p^r(\mathbf{x})f_r(\mathbf{x}) + \mathbf{r}^T \nabla_{\mathbf{x}} f_r(\mathbf{x})] \\ &= \mathbb{E}_q[(s_p^r(\mathbf{x}) - s_q^r(\mathbf{x}))f_r(\mathbf{x})] \end{aligned}$$

Then, we can upper bound the PSD (Eq.9) as the following

$$\begin{aligned} & \sum_{r \in O_r} \mathbb{E}_q[(s_p^r(\mathbf{x}) - s_q^r(\mathbf{x}))f_r(\mathbf{x})] \\ & \leq \sum_{r \in O_r} \sqrt{\mathbb{E}_q[(s_p^r(\mathbf{x}) - s_q^r(\mathbf{x}))^2]} \sqrt{\mathbb{E}_q[(f_r(\mathbf{x}))^2]} \end{aligned}$$

by Cauchy-Schwarz inequality. It is well-known that the equality holds when $f_r(\mathbf{x}) \propto (s_p^r(\mathbf{x}) - s_q^r(\mathbf{x}))$ \square

F.2. Proof of Theorem 3

Proof. The key to this proof is to notice that $h_{r_{g_r}}^*$ is the conditional mean of f_r^* w.r.t. the transformed distribution q_{G_r} . By using the similar terminology of proposition 1, and let $s_p^r = s_p^r(\mathbf{x})$ for abbreviation. Then,

$$\begin{aligned} & \mathbb{E}_q[(s_p^r - s_q^r)f_r^*(\mathbf{x})] - \mathbb{E}_q[(s_p^r - s_q^r)h_{r_{g_r}}^*(\mathbf{x}^T \mathbf{g}_r)] \\ & = \int q(\mathbf{x})[(s_p^r - s_q^r)^2 - (s_p^r - s_q^r)h_{r_{g_r}}^*(\mathbf{x}^T \mathbf{g}_r)]d\mathbf{x} \\ & = \int q_{G_r}(y_d) \left[\int q_{G_r}(\mathbf{y}_{-d}|y_d)(s_p^r(\mathbf{G}_r^{-1}\mathbf{y}) - s_q^r(\mathbf{G}_r^{-1}\mathbf{y}))^2 d\mathbf{y}_{-d} \right. \\ & \quad \left. - \int q_{G_r}(s_p^r(\mathbf{G}_r^{-1}\mathbf{y}) - s_q^r(\mathbf{G}_r^{-1}\mathbf{y}))d\mathbf{y}_{-d} h_{r_{g_r}}^*(y_d) \right] dy_d \\ & = \int q_{G_r}(y_d) \left[\int q_{G_r}(\mathbf{y}_{-d}|y_d)(f_r^*(\mathbf{G}_r^{-1}\mathbf{y}) - h_{r_{g_r}}^*(y_d))^2 d\mathbf{y} \right. \\ & \quad \left. - \mathbb{E}_q[(f_r^*(\mathbf{x}) - h_{r_{g_r}}^*(\mathbf{x}^T \mathbf{g}_r))^2] \right] \geq 0 \end{aligned}$$

where the 3rd equality is due to the fact that $h_{r_{g_r}}^*$ is the conditional mean of f_r^* . Thus,

$$\begin{aligned} & PSD - S_{g_r} \\ & = \sum_{r \in O_r} \mathbb{E}_q[(s_p^r - s_q^r)f_r^*(\mathbf{x})] - \mathbb{E}_q[(s_p^r - s_q^r)h_{r_{g_r}}^*(\mathbf{x}^T \mathbf{g}_r)] \\ & = \sum_{r \in O_r} \mathbb{E}_q[(f_r^*(\mathbf{x}) - h_{r_{g_r}}^*(\mathbf{x}^T \mathbf{g}_r))] \geq 0 \end{aligned}$$

\square

F.3. Proof of Theorem 4

Before we give the details, we introduce the main inequality and its variant for the proof.

Lemma 3 (Poincaré Inequality). *For a probabilistic distribution p that satisfies assumption 7, for all locally Lipschitz function $f(\mathbf{x}) : \mathcal{X} \subseteq \mathbb{R}^D \rightarrow \mathbb{R}$, we have the following inequality*

$$\text{Var}_p(f(\mathbf{x})) \leq C_p \int p(\mathbf{x}) \|\nabla_{\mathbf{x}} f(\mathbf{x})\|^2 d\mathbf{x}$$

where C_p is called Poincaré constant that is only related to p .

One should note that the assumption of log concavity of p is a sufficient condition for Poincaré inequality, which means it may be applied to a broader class of distributions. But it is beyond the scope of this work.

Due to the form of optimal test functions of *SSD-g*, we need to deal with the transformed distribution q_{G_r} and its conditional expectations (see Eq.8). Unfortunately, the original form of Poincaré inequality cannot be applied. In the following, we introduce its variant called *subspace* Poincaré inequality (Constantine et al., 2014; Zahm et al., 2020; Parante et al., 2020) to deal with the conditional expectation. But before that, we need to make sure the transformed distribution and its conditional density still satisfy the conditions of Poincaré inequality, i.e. log concavity.

Lemma 4 (Preservation of log concavity). *Assume distribution $q(\mathbf{x}) = \exp(-V(\mathbf{x}))$ is log-concave. With arbitrary orthogonal matrix \mathbf{G} and corresponding transformed distribution $q_G(\mathbf{y}_{-d} | y_d)$ is also log-concave for all $d = 1, \dots, D$.*

Proof. Assume we have $\mathbf{y} = \mathbf{G}\mathbf{x}$. Thus, by change of variable formula, $q_G(\mathbf{y}) = q(\mathbf{x}) = q(\mathbf{G}^{-1}\mathbf{y}) = \exp(-V(\mathbf{G}^{-1}\mathbf{y}))$. Thus, the log conditional distribution

$$\log q_G(\mathbf{y}_{-d} | y_d) = -V(\mathbf{G}^{-1}\mathbf{y}) - \log q_G(y_d)$$

We inspect its Hessian w.r.t \mathbf{y}_{-d}

$$\begin{aligned} & \nabla_{\mathbf{y}_{-d}}^2 (V(\mathbf{G}^{-1}\mathbf{y}) + \log q_G(y_d)) \\ & = \nabla_{\mathbf{y}_{-d}}^2 (V(\mathbf{G}^{-1}\mathbf{y})) \\ & = \nabla_{\mathbf{y}_{-d}} (\mathbf{G}_{\setminus d} V'(\mathbf{G}^{-1}\mathbf{y})) \\ & = \mathbf{G}_{\setminus d} V''(\mathbf{G}^{-1}\mathbf{y}) \mathbf{G}_{\setminus d}^T \end{aligned}$$

where $\mathbf{G}_{\setminus d} = [\mathbf{g}_1, \dots, \mathbf{g}_{d-1}, \mathbf{g}_{d+1}, \dots, \mathbf{g}_D]^T$ and $V'(\mathbf{G}^{-1}\mathbf{y}) = \nabla_{\mathbf{G}^{-1}\mathbf{y}} V(\mathbf{G}^{-1}\mathbf{y})$. We already know that $V(\cdot)$ is a convex function. Thus, for all $\mathbf{u} \in \mathbb{R}^D$, $\mathbf{u}^T V''(\mathbf{x}) \mathbf{u} \geq 0$, therefore,

$$\mathbf{u}^T \mathbf{G}_{\setminus d} V''(\mathbf{G}^{-1}\mathbf{y}) \mathbf{G}_{\setminus d}^T \mathbf{u} = \mathbf{l}^T V''(\mathbf{G}^{-1}\mathbf{y}) \mathbf{l} \geq 0$$

where $\mathbf{l} = \mathbf{G}_{\setminus d}^T \mathbf{u}$. \square

Now, we can introduce the subspace Poincaré inequality

Lemma 5 (Poincaré inequality for conditional expectation). *Assume the assumption 2,4 (density regularity), 7 (Poincaré inequality condition) are satisfied, with arbitrary orthogonal matrix \mathbf{G} , $\mathbf{y} = \mathbf{G}\mathbf{x}$ and $y_d = \mathbf{x}^T \mathbf{g}_d$, we have the following inequality*

$$\begin{aligned} & \int q_G(\mathbf{y}_{-d} | y_d) [f_r^*(\mathbf{G}^{-1}\mathbf{y}) - h_{r_{g_r}}^*(y_d)]^2 d\mathbf{y}_{-d} \\ & \leq C_{y_d} \mathbb{E}_{q_G(\mathbf{y}_{-d}|y_d)} \left[\|\mathbf{G}_{\setminus d} \nabla f_r^*\|^2 \right] \end{aligned}$$

where C_{y_d} is the Poincaré constant, $\mathbf{G}_{\setminus d} = [\mathbf{a}_1, \dots, \mathbf{a}_{d-1}, \mathbf{a}_{d+1}, \dots, \mathbf{a}_D]^T$ is the orthogonal matrix \mathbf{G} excluding $\mathbf{a}_d = \mathbf{g}$ and f_r^*, h_{r, g_r}^* are the optimal test functions defined in proposition 4, 1 respectively with coefficient 1.

Proof. From lemma 4, we know $q_G(\mathbf{y}_{-d} | y_d)$ is a log-concave distribution. Therefore, it satisfies the Poincaré inequality (lemma.3). We have

$$\begin{aligned} & \int q_G(\mathbf{y}_{-d} | y_d) [f_r^*(\mathbf{G}^{-1}\mathbf{y}) - h_{r, g_r}^*(y_d)]^2 d\mathbf{y}_{-d} \\ &= \text{Var}_{q_G(\mathbf{y}_{-d}|y_d)}(f_r^*(\mathbf{G}^{-1}\mathbf{y})) \\ &\leq C_{y_d} \int q_G(\mathbf{y}_{-d} | y_d) \|\nabla_{\mathbf{y}_{-d}} f_r^*(\mathbf{G}^{-1}\mathbf{y})\|^2 d\mathbf{y}_{-d} \\ &= C_{y_d} \int q_G(\mathbf{y}_{-d} | y_d) \|\mathbf{G}_{\setminus d} \nabla_{\mathbf{G}^{-1}\mathbf{y}} f_r^*(\mathbf{G}^{-1}\mathbf{y})\|^2 d\mathbf{y}_{-d} \end{aligned}$$

The first equality comes from the fact that $h_{r, g_r}^*(y_d)$ is actually a conditional mean of $f_r^*(\mathbf{G}^{-1}\mathbf{y})$, and the inequality comes from the direct application of Poincaré inequality on $q_G(\mathbf{y}_{-d}|y_d)$ and $f_r^*(\mathbf{G}^{-1}\mathbf{y})$. \square

With the above tools, it is now easy to prove theorem 4.

Theorem 4

Proof. We can re-write the inner part of controlled approximation (Eq.11) in the following:

$$\begin{aligned} & \int q_{G_r}(y_d, \mathbf{y}_{-d}) [f_r^*(\mathbf{G}_r^{-1}\mathbf{y}) - h_{r, g_r}^*(y_d)]^2 d\mathbf{y} \\ &= \int q_{G_r}(y_d) \mathbb{E}_{q_{G_r}(\mathbf{y}_{-d}|y_d)} [(f_r^*(\mathbf{G}_r^{-1}\mathbf{y}) - h_{r, g_r}^*(y_d))^2] d\mathbf{y} \\ &\leq \int q_{G_r}(y_d, \mathbf{y}_{-d}) C_{y_d} \|\mathbf{G}_{r \setminus d} \nabla f_r^*\|^2 d\mathbf{y} \\ &\leq C_{sup} \int q_{G_r}(y_d, \mathbf{y}_{-d}) \|\mathbf{G}_{r \setminus d} \nabla f_r^*\|^2 d\mathbf{y} \\ &= C_{sup} \int q(\mathbf{x}) \text{tr} \left[(\mathbf{G}_{r \setminus d} \nabla f_r^*) (\mathbf{G}_{r \setminus d} \nabla f_r^*)^T \right] d\mathbf{x} \\ &= C_{sup} \text{tr} \left[\mathbf{G}_{r \setminus d} \mathbf{H}_r \mathbf{G}_{r \setminus d}^T \right] \end{aligned}$$

where the first inequality is directly from lemma 5 and the second inequality is from the definition of C_{sup} .

To minimize this upper bound, we can directly use the theorem 2.1 (Sameh & Tong, 2000) by setting $B = I$ and $\mathbf{X} = \mathbf{G}_{r \setminus d}^T$. Therefore, we only need to check if $\mathbf{G}_{r \setminus d} \mathbf{G}_{r \setminus d}^T = I$. This is trivial as \mathbf{G}_r is an orthogonal matrix. Thus, the proof is complete. \square

G. Theory related to active slice r

G.1. Proof of proposition 2

First, from the theorem 3, we have

$$\text{PSD}_r \geq S_{r, g}$$

Thus, we can establish the following lower bound

$$\begin{aligned} & S_{r_1, g_{r_1}} - S_{r_2, g_{r_2}} \\ &\geq S_{r_1, g_{r_1}} - \text{PSD}_{r_2} \\ &= \underbrace{S_{r_1, g_{r_1}} - \text{PSD}_{r_1}}_{\text{controlled approximation}} + \text{PSD}_{r_1} - \text{PSD}_{r_2} \end{aligned}$$

Thus, from theorem 4, we can obtain

$$\begin{aligned} & S_{r_1, g_{r_1}} - \text{PSD}_{r_1} \\ &= -\mathbb{E}_q \left[(f_{r_1}^*(\mathbf{x}) - h_{r_1, g_{r_1}}^*(\mathbf{x}^T \mathbf{g}_{r_1}))^2 \right] \\ &\geq -C_{\text{sup}} \text{tr}(\mathbf{G}_{r_1 \setminus d} \mathbf{H}_{r_1} \mathbf{G}_{r_1 \setminus d}^T) \\ &= -C_{\text{sup}} \text{tr}(\mathbf{H}) + \underbrace{\mathbf{g}_{r_1}^T \mathbf{H}_{r_1} \mathbf{g}_{r_1}}_{\geq 0} \\ &\geq -C_{\text{sup}} \text{tr}(\mathbf{H}_{r_1}) \end{aligned}$$

where the first inequality is from the upper bound of controlled approximation (theorem 4) and $\mathbf{g}_{r_1}^T \mathbf{H}_{r_1} \mathbf{g}_{r_1} \geq 0$ is due to the positive semi-definiteness of \mathbf{H}_{r_1} . Assume we have an orthogonal basis O_{r_1} that contains \mathbf{r}_1 , thus, for each $\mathbf{r} \in O_{r_1}$, we have $\text{tr}(\mathbf{H}_r) \geq 0$. Then, we can show

$$\begin{aligned} \text{tr}(\mathbf{H}_{r_1}) &\leq \sum_{\mathbf{r} \in O_{r_1}} \text{tr}(\mathbf{H}_r) \\ &= \sum_{\mathbf{r} \in O_{r_1}} \text{tr}(\mathbb{E}_q[\nabla_{\mathbf{x}} \mathbf{f}^*(\mathbf{x}) \mathbf{r} \mathbf{r}^T \nabla_{\mathbf{x}} \mathbf{f}^*(\mathbf{x})^T]) \\ &= \text{tr}(\mathbb{E}_q[\nabla_{\mathbf{x}} \mathbf{f}^*(\mathbf{x}) \sum_{\mathbf{r} \in O_{r_1}} \mathbf{r} \mathbf{r}^T \nabla_{\mathbf{x}} \mathbf{f}^*(\mathbf{x})^T]) \\ &= \text{tr}(\mathbb{E}_q[\nabla_{\mathbf{x}} \mathbf{f}^*(\mathbf{x}) \nabla_{\mathbf{x}} \mathbf{f}^*(\mathbf{x})^T]) \\ &= \sum_{i=1}^D \omega_i = \Omega \end{aligned}$$

where $\{\omega_i\}_i^D$ are the eigenvalues of $\mathbb{E}_q[\nabla_{\mathbf{x}} \mathbf{f}^*(\mathbf{x}) \nabla_{\mathbf{x}} \mathbf{f}^*(\mathbf{x})^T]$, $\mathbf{f}^*(\mathbf{x}) = \mathbf{s}_p(\mathbf{x}) - \mathbf{s}_q(\mathbf{x})$ and $\sum_{\mathbf{r} \in O_{r_1}} \mathbf{r} \mathbf{r}^T = I$ since $\mathbf{r} \in O_{r_1}$ are orthogonal to each other.

Thus, we can substitute it back, we have

$$S_{r_1, g_{r_1}} - S_{r_2, g_{r_2}} \geq \text{PSD}_{r_1} - \text{PSD}_{r_2} - C_{\text{sup}} \Omega$$

G.2. Proof of theorem 5

Proof. From proposition 4 we know $f_r^*(\mathbf{x}) = (s_p^r(\mathbf{x}) - s_q^r(\mathbf{x}))$, thus, we can substitute into PSD

(Eq.9), we get

$$\text{PSD}_r = \max_{\mathbf{r} \in \mathbb{S}^{D-1}} \mathbb{E}_q \left[\left((\mathbf{s}_p(\mathbf{x}) - \mathbf{s}_q(\mathbf{x}))^T \mathbf{r} \right)^2 \right]$$

To maximize it, we consider the following constraint optimization problem.

$$\max_{\mathbf{r}} \mathbb{E}_q \left[\left((\mathbf{s}_p(\mathbf{x}) - \mathbf{s}_q(\mathbf{x}))^T \mathbf{r} \right)^2 \right] \quad \text{s.t.} \quad \|\mathbf{r}\|^2 = 1$$

We take the derivative of the corresponding Lagrange multiplier w.r.t. \mathbf{r} ,

$$\begin{aligned} & \mathbb{E}_q \left[\nabla_{\mathbf{r}} \left((\mathbf{s}_p(\mathbf{x}) - \mathbf{s}_q(\mathbf{x}))^T \mathbf{r} \right)^2 \right] - 2\lambda \mathbf{r} = 0 \\ \Rightarrow & \mathbb{E}_q \left[(\mathbf{s}_p(\mathbf{x}) - \mathbf{s}_q(\mathbf{x}))^T \mathbf{r} (\mathbf{s}_p(\mathbf{x}) - \mathbf{s}_q(\mathbf{x})) \right] = \lambda \mathbf{r} \\ \Rightarrow & \underbrace{\mathbb{E}_q \left[(\mathbf{s}_p(\mathbf{x}) - \mathbf{s}_q(\mathbf{x})) (\mathbf{s}_p(\mathbf{x}) - \mathbf{s}_q(\mathbf{x}))^T \right]}_{\mathbf{S} = \mathbb{E}_q[f^*(\mathbf{x})f^{*T}(\mathbf{x})]} \mathbf{r} = \lambda \mathbf{r} \\ \Rightarrow & \mathbf{S} \mathbf{r} = \lambda \mathbf{r} \end{aligned}$$

This exactly the problem of finding eigenpair for matrix \mathbf{S} . Let's assume $\mathbf{r} = \mathbf{v}$ which is the eigenvector of \mathbf{S} with corresponding eigenvalue λ . Substituting it back to PSD , we have

$$\begin{aligned} & \mathbb{E}_q \left[\left((\mathbf{s}_p(\mathbf{x}) - \mathbf{s}_q(\mathbf{x}))^T \mathbf{r} \right)^2 \right] \\ = & \mathbb{E}_q \left[(\mathbf{s}_p(\mathbf{x}) - \mathbf{s}_q(\mathbf{x}))^T \mathbf{r} (\mathbf{s}_p(\mathbf{x}) - \mathbf{s}_q(\mathbf{x})) \right]^T \mathbf{r} \\ = & \mathbf{r}^T \mathbf{S} \mathbf{r} \\ = & \lambda \mathbf{v}^T \mathbf{v} = \lambda \end{aligned}$$

Thus, to obtain the active slice \mathbf{r} , we only need to find the eigenvector of \mathbf{S} with the largest eigenvalue. \square

G.3. Greedy algorithm is eigen-decomposition

Corollary 6.2 (Greedy algorithm is eigen-decomposition). *Assume the conditions in theorem 5 are satisfied, then finding the orthogonal basis O_r from the greedy algorithm is equivalent to the eigen-decomposition of \mathbf{S} .*

Proof. Assume we have obtained the active slice \mathbf{r} from theorem 5, thus, we have $\mathbf{S} \mathbf{r} = \lambda \mathbf{r}$. The greedy algorithm for \mathbf{r}' can be translated into the following constrained optimization

$$\begin{aligned} & \max_{\mathbf{r}'} \mathbb{E}_q \left[\left((\mathbf{s}_p(\mathbf{x}) - \mathbf{s}_q(\mathbf{x}))^T \mathbf{r}' \right)^2 \right] \\ \text{s.t.} & \quad \|\mathbf{r}'\|^2 = 1 \\ & \quad \mathbf{r}'^T \mathbf{r}' = 0 \end{aligned}$$

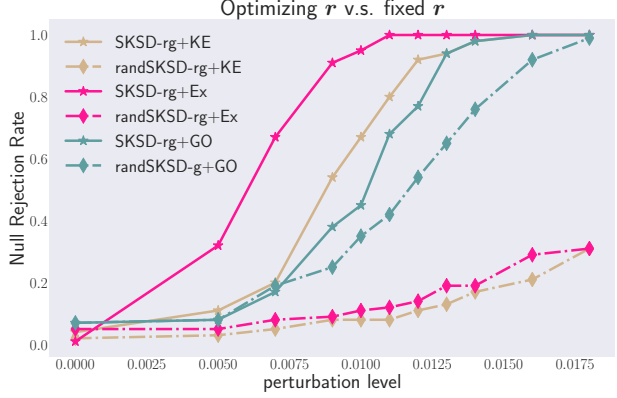


Figure 5. The test power difference with good \mathbf{r} and fixed \mathbf{r} .

By using Lagrange multipliers (μ, γ) , and then take derivative w.r.t. \mathbf{r}' ,

$$\mathbf{S} \mathbf{r}' = \mu \mathbf{r}' + \gamma \mathbf{r}$$

Then taking the inner product with \mathbf{r} in both side, and notice \mathbf{S} is a symmetric matrix, we obtain

$$\begin{aligned} \gamma &= \langle \mathbf{S} \mathbf{r}', \mathbf{r} \rangle \\ &= \langle \mathbf{r}', \mathbf{S}^T \mathbf{r} \rangle \\ &= \langle \mathbf{r}', \lambda \mathbf{r} \rangle = 0 \end{aligned}$$

Therefore, the constrained optimization is the same as the one in theorem 5, which is to find a eigenvector of \mathbf{S} that is different from \mathbf{r} . Repeat the above procedure, the final resulting O_r is a group of eigenvectors of \mathbf{S} . \square

H. Experiment Details

For all experiments in this paper, we use RBF kernel with median heuristics.

H.1. Benchmark GOF test

For gradient based optimization, we use Adam (Kingma & Ba, 2014) with learning rate 0.001 and $\beta = (0.9, 0.99)$. We use random initialization for SKSD-g+GO by drawing \mathbf{g}_r from a Gaussian distribution before normalizing them to unit vectors. For kernel smooth and gradient estimator, we use RBF kernel with median heuristics. Although the algorithm 1 states that small Gaussian noise are needed for active slices, in practice, we found that active slices still have the satisfactory performance without the noise.

The significance level for GOF test $\alpha = 0.05$, and the dimensions of the benchmark problems grow from 2 to 100. We use 1000 bootstrap samples to estimate the threshold and run 100 trials for each benchmark problems.

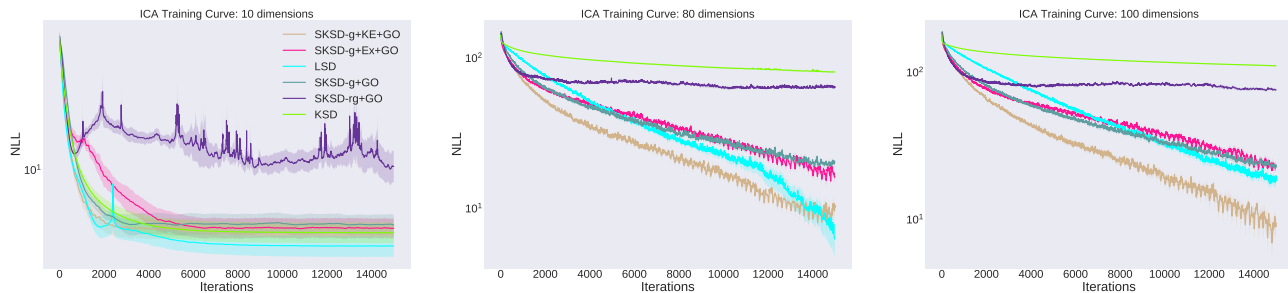


Figure 6. Training curve of ICA model with test NLL for different dimensions.

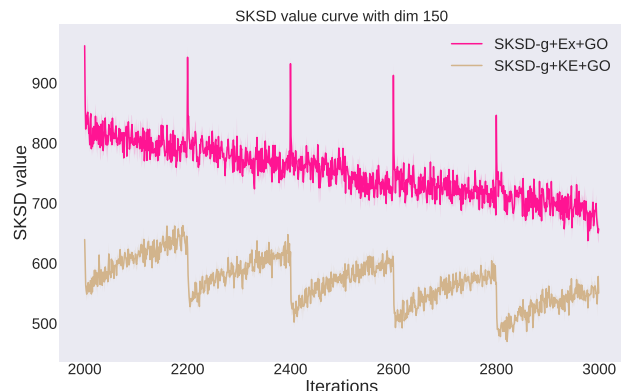


Figure 7. SKSD value curve with 150 dimensional ICA during iteration 5000 to 6000

H.2. RBM GOF test

We set significance level $\alpha = 0.05$ and use 1000 bootstrap samples to compute the threshold. For methods that require training (*SKSD* based method), we need to collect some training samples. Following the same settings as (Gong et al., 2021), to avoid over-fitting to small training set, we collect the pseudo-samples during the early burn-in stage. Note that these pseudo-samples should not be used for testing, as they are not drawn from the q . We collect 2000 samples. For gradient based optimization, we use the same optimizer as benchmark GOF test with the same hyper-parameters. The batch size is 100. For initialization of *SKSD+GO*, we found that if the slices are initialized randomly, the gradient optimization fails to find meaningful slices within a reasonable amount of time, therefore, we have initialize the \mathbf{r} and \mathbf{g}_r as one-hot vectors and set $\mathbf{r} = \mathbf{g}_r$. For pruning ablation study, if the pruning level is set to 50, we initialize \mathbf{r} and \mathbf{g}_r to be the identity matrix. The default number of gradient optimization for *SKSD+GO* is 50. For active slice method, we directly use the active slices without any further optimizations. We run 100 trials for GOF test with 1000 test samples per trial.

(Gong et al., 2021) reports *SKSD-rg+GO* has near optimal test power at perturbation level 0.01. The performance difference is because they train the *SKSD-rg* with 200 batch sizes per burn-in step. Namely, the training set size are $200 \times 2000 = 400000$, which is 200 times larger than ours. They also run 2000 iterations, which is equivalent to 100 epochs in our settings.

Figure 5 shows the test power difference with optimized \mathbf{r} and fixed \mathbf{r} . The legend with *rand* annotation implies we randomly initialized \mathbf{r} as one-hot vectors and fix them while updating \mathbf{g}_r using *GO* or active slice. Without *rand*, it means both \mathbf{r} and \mathbf{g}_r are optimized. We only use 3 \mathbf{r} for active slice method and 50 for gradient-based counterpart. For active slice method with pruning (*randSKSD-g+Ex* or *randSKSD-g+KE*), despite we show that any finite random slices define a valid discrepancy, it is clear that the performance is quite poor with random initialized \mathbf{r} 's. It indicates that using active slices of \mathbf{g}_r alone cannot compensate the poor discriminating power of the random \mathbf{r} 's. Although *SKSD-rg+GO* demonstrates an advantage compared to *randSKSD-g+GO*, the performance boost is less clear compared to active slices method. This is because we do not use any pruning for *randSKSD-g+GO*, and adopt orthogonal basis $O_r = \mathbf{I}$. Despite the orthogonal basis may not capture the important directions, they can provide reasonable discriminating power due to their orthogonality from each other. In summary, using good directions for \mathbf{r} is advantageous compared to fixed \mathbf{r} .

H.3. Model learning: Training ICA

We use Adam optimizer for the model and slice directions with learning rate 0.001 and $\beta = (0.9, 0.99)$. We totally run 15000 iterations. The batch size is 100. We evaluate our method in dimension 10, 80, 100 and 150. For more stable comparisons, we initialized the weight matrix \mathbf{W} until its conditional number is smaller than its dimensions. For active slice method, we use randomly sampled 3000 data from training set to estimate the score difference and the matrices used for eigen-decomposition.

For *SKSD-rg+GO*, we initialize the \mathbf{r} to be a group of one-

hot vectors to form identity matrix and $\mathbf{g}_r = \mathbf{r}$. We use an adversarial training procedure that updates both \mathbf{r} and \mathbf{g}_r using Adam once per iteration before we update the model. For *SKSD-g+GO*, we fix the orthogonal basis O_r to be the identity matrix and only update \mathbf{g}_r . Each results are the average of 5 runs of training.

As for the reason why *SKSD-g+Ex+GO* performs worse than *+KE+GO*, we suspect that *+Ex* only focus on directions with high discriminating power. However, high discriminating power is not necessarily good for model learning. It may focus on very small area that is different from the target but ignore the larger area with small difference. Because our algorithm for finding basis is greedy, this means it can ignore the generally good directions if they are not orthogonal to the directions with high discriminating power.

From figure 7, we can observe there is a spike of *SKSD-g+Ex+GO* value at every 200 iterations due to the new active slices found at the beginning of each training epoch. However, the value drops significantly fast to the one before new active slices. This indicates the *Ex* indeed finds directions with large discriminating power but they do not represents good directions for learning due to the fast drop of SKSD values. On the other hand, the directions provided by KE does not give the highest discriminating power, but it can find generally good directions of \mathbf{g}_r using *GO* refinement steps within a few iterations. This means the directions found by *KE* indeed represents good directions for learning as the model cannot decrease this value quickly. We guess this is due to the smooth estimation of KE, where very small areas with high discriminating power are smoothed out.

Figure 6 shows the ICA training curve of other dimensions. We can observe the convergence speed of LSD deteriorates as the dimension increases due to the poor test function in early training stage, whereas *SKSD-g+KE+GO* maintains the fastest convergence in high dimensions.

I. Perturbation of eigenvectors

The active slice method (algorithm 1) is mainly based on the eigenvalue-decomposition of matrix \mathbf{H} , where

$$\mathbf{H} = \int q(\mathbf{x}) \nabla_{\mathbf{x}} f_r^*(\mathbf{x}) \nabla_{\mathbf{x}} f_r^*(\mathbf{x})^T d\mathbf{x}$$

Obtaining the analytic form of \mathbf{H} involves complicated integration, so Monte Carlo estimation is often used for approximation. We denote it as $\hat{\mathbf{H}}$, with M being the number of samples:

$$\hat{\mathbf{H}} = \frac{1}{M} \sum_{i=1}^M [\nabla_{\mathbf{x}_i} f_r^*(\mathbf{x}_i) \nabla_{\mathbf{x}_i} f_r^*(\mathbf{x}_i)^T] \quad (53)$$

Let \mathbf{g} be the top eigenvector of \mathbf{H} and $\hat{\mathbf{g}}$ be the top eigen-

vector of $\hat{\mathbf{H}}$. Let λ_1, λ_2 be the top two eigenvalues of \mathbf{H} . Assuming the error matrix $\mathbf{E} = \hat{\mathbf{H}} - \mathbf{H}$ is deterministic, (Yu et al., 2015) proved that

$$\|\mathbf{g}\mathbf{g}^T(\mathbf{I} - \hat{\mathbf{g}}\hat{\mathbf{g}}^T)\|_F \leq \frac{2\|\mathbf{E}\|_{op}}{\lambda_1 - \lambda_2} \quad (54)$$

where we define the operator norm for a given $n \times n$ matrix \mathbf{A} as

$$\|\mathbf{A}\|_{op} = \sup\{\|\mathbf{A}\mathbf{x}\| : \mathbf{x} \in \mathbb{R}^n \text{ with } \|\mathbf{x}\| = 1\}$$

We also have (with proof below)

$$\min_{\epsilon \in \{-1, 1\}} \|\mathbf{g} - \epsilon \hat{\mathbf{g}}\|_2 \leq \sqrt{2} \|\mathbf{g}\mathbf{g}^T(\mathbf{I} - \hat{\mathbf{g}}\hat{\mathbf{g}}^T)\|_F \quad (55)$$

Inequality 54 and 55 imply that,

$$\min_{\epsilon \in \{-1, 1\}} \|\mathbf{g} - \epsilon \hat{\mathbf{g}}\|_2 \leq 2^{3/2} \frac{\|\hat{\mathbf{H}} - \mathbf{H}\|_{op}}{\lambda_1 - \lambda_2} \quad (56)$$

I.1. Proof of inequality 55

Proposition 5. *Let \mathbf{S} and \mathbf{U} be two matrices with orthonormal columns and equal rank r . Let $\mathbf{\Pi}_S$ (resp. $\mathbf{\Pi}_U$) indicates the projection matrix to the column space of \mathbf{S} (resp. \mathbf{U}). Then*

$$\min_{O \in \mathbb{R}^{r \times r} \text{ orthogonal}} \|\mathbf{S} - \mathbf{U}\mathbf{O}\|_F \leq \sqrt{2} \|\mathbf{\Pi}_S(\mathbf{I} - \mathbf{\Pi}_U)\|_F \quad (57)$$

When $r = 1$, we denote \mathbf{O} as ϵ . Following the definition of orthogonal matrix, we have $\epsilon^T \epsilon = \epsilon^2 = 1$, hence $\epsilon \in \{-1, 1\}$. Substituting $\mathbf{S} = \mathbf{g}$ and $\mathbf{U} = \hat{\mathbf{g}}$, we get inequality 55.

Proof. Let $\mathbf{W}\mathbf{\Sigma}\mathbf{V}^T$ be a singular value decomposition of $\mathbf{S}^T\mathbf{U}$, and use $\mathbf{O} = \mathbf{V}\mathbf{W}^T$. Now,

$$\begin{aligned} \|\mathbf{S} - \mathbf{U}\mathbf{O}\|_F^2 &= \text{Tr}((\mathbf{S} - \mathbf{U}\mathbf{O})^T(\mathbf{S} - \mathbf{U}\mathbf{O})) \\ &= \|\mathbf{S}\|_F^2 + \|\mathbf{U}\|_F^2 - 2\text{Tr}(\mathbf{O}\mathbf{S}^T\mathbf{U}) \\ &= 2r - 2\text{Tr}(\mathbf{\Sigma}) \end{aligned}$$

where r is the rank of \mathbf{S} and \mathbf{U} . On the other hand, by Pythagora's theorem

$$\begin{aligned} \|\mathbf{\Pi}_S(\mathbf{I} - \mathbf{\Pi}_U)\|_F^2 &= \|\mathbf{\Pi}_S\|_F^2 - \|\mathbf{\Pi}_S\mathbf{\Pi}_U\|_F^2 \\ &= r - \|\mathbf{\Pi}_S\mathbf{\Pi}_U\|_F^2 \\ &= r - \|\mathbf{S}\mathbf{S}^T\mathbf{U}\mathbf{U}^T\|_F^2 \\ &= r - \text{Tr}(\mathbf{\Sigma}^2) \end{aligned}$$

We claim that the entries of $\mathbf{\Sigma}$ are bounded above by 1, such that $\text{Tr}(\mathbf{\Sigma}) \leq \text{Tr}(\mathbf{\Sigma}^2)$, then

$$\begin{aligned} \min_{O \in \mathbb{R}^{r \times r} \text{ orthogonal}} \|\mathbf{S} - \mathbf{U}\mathbf{O}\|_F^2 &\leq 2r - 2\text{Tr}(\mathbf{\Sigma}) \\ &\leq 2r - 2\text{Tr}(\mathbf{\Sigma}^2) \\ &= 2\|\mathbf{\Pi}_S(\mathbf{I} - \mathbf{\Pi}_U)\|_F^2 \end{aligned}$$

Taking the square root of both sides yields the desired inequality. To prove the claim, let $\omega = [\mathbf{S}, \mathbf{S}']$ and $\tilde{\mathbf{U}} = [\mathbf{U}, \mathbf{U}']$ be orthogonal matrices. Then $\mathbf{S}^T \mathbf{U}$ is a diagonal block in $\omega^T \tilde{\mathbf{U}}$. It follows that $\max_i \Sigma_{i,i} = \|\mathbf{S}^T \mathbf{U}\|_{op} \leq \|\omega^T \tilde{\mathbf{U}}\|_{op} = 1$ \square

From Eq.56, we can see if the top two eigenvalues are similar, then their corresponding eigenvectors can be arbitrary different. In terms of our active slice algorithm, it means if the most discriminating directions for two distributions q, p have similar "magnitude of difference", our algorithm may fail under Monte-carlo approximation. On the other hand, if the eigenvalues are different, Eq.56 guarantees that eigenvectors from $\hat{\mathbf{H}}$ are not far-away from the truth.